Title
Effects of number of electric vehicles charging/discharging on total electricity costs in commercial buildings with time-of-use energy and demand charges

Journal
Journal of Renewable and Sustainable Energy, 14(3)

ISSN
1941-7012

Authors
Ghosh, Avik
Zapata, Mónica Zamora
Silwal, Sushil
et al.

Publication Date
2022-05-01

DOI
10.1063/5.0086924

Effects of number of electric vehicles charging/discharging on total electricity costs in commercial buildings with time-of-use energy and demand charges

Avik Ghosh*, Mónica Zamora Zapata, Sushil Silwal, Adil Khurram, Jan Kleissl

Department of Mechanical and Aerospace Engineering, University of California, San Diego, CA 92093-0411, United States

*Corresponding author
Email address: avghosh@eng.ucsd.edu

Abstract

Electric vehicle (EV) penetration has been increasing in the modern electricity grid and has been complemented by the growth of EV charging infrastructure. This paper addresses the gap in the literature on the EV effects of total electricity costs in commercial buildings by incorporating V0G, V1G, and V2B charging. The electricity costs are minimized in 14 commercial buildings with real load profiles, demand and energy charges. The scientific contributions of this study are the incorporation of demand charges, quantification of EV and smart charging electricity costs and benefits using several representative long-term datasets, and the derivation of approximate equations that simplify the estimation of EV economic impacts. Our analysis is primarily based on an idealized uniform EV commuter fleet case study. The V1G and V2B charging electricity costs as a function of the number of EVs initially diverge with increasing charging demand and then become parallel to one another with the V2B electricity costs being lower than V1G costs. A longer EV layover time leads to higher numbers of V2B charging stations that can be installed such that original (pre-EV) electricity costs are not exceeded, as compared to a shorter layover time. Sensitivity analyses based on changing the final SOC of EVs between 90% to 80% and initial SOC between 50 to 40% (thereby keeping charging energy demand constant) show that the total electricity costs are the same for V0G and V1G charging, while for V2B charging the total electricity costs decrease as final SOC decreases.

Keywords: Demand charge; Smart charging; Electric vehicles; Buildings; Electricity cost minimization; Optimization

Nomenclature

BC	EV battery capacity (kWh)	R	rate of energy charges (\$/kWh) / rate of demand charges (\$/kW)
BE	EV battery energy (kWh)	RT	regularization term
CD	EV charging demand (kWh)	SOC	EV state of charge
d	date index of month	t	time (hours)
EC	energy charges (\$)	Δt	time resolution (hours)

ED	energy demand (kWh)	w	weight
EV	electric vehicle / electric vehicle charging rate (kW)	wf	weighing factor for regularization term
j	EV index	*Subscripts*	
L	original (pre-EV) building load (kW)	cor	corrected
m	number of days in a month	day	daily
n	total number of EVs	end	end of simulation time
NC	non-coincident	f	final
NCDC	non-coincident demand charge ($)	i	initial
NCDP	non-coincident demand peak (kW)	off	off-peak layover period
NL	optimized net load of buildings (kW)	on	on-peak layover period
OC	other charges ($)	opt	optimum
OPDC	on-peak period demand charge ($)	org	original
OPDP	on-peak period demand peak (kW)	thr	threshold
PP	on-peak period		

1. Introduction

1.1 Motivation

The use of electric vehicles (EVs) has significantly increased in the past decade and is projected to increase even more in the coming decade. The push towards the increasing market penetration of EVs has also been complemented by the strong growth of EV charging infrastructure along interstate highways, at workplaces, and at public parking lots [1]. There are three popular types of EV charging: V0G ("dumb" charging at constant full power from when the vehicles are plugged in until they are unplugged or full, whichever occurs earlier), V1G (unidirectional, grid-to-vehicle variable smart charging) and V2G (bidirectional, grid-to-vehicle and vehicle-to-grid variable smart charging). V2B (bidirectional, grid-to-vehicle and vehicle-to-building variable smart charging) is a variant of V2G, where the EVs, instead of feeding back energy directly to the grid, reduce the building's net load peak (grid import). Smart charging optimally charges and discharges (in case of V2G/V2B) the EVs to provide economic benefit to EV owners, microgrid/EV charging station operators, and/or grid operators [2].

1.2 Literature Review

V2G chargers are gaining importance and making a stronger business case because of value streams associated with operational flexibility as compared to V1G chargers [3]. While the EV charging literature is vast, the following literature in this paragraph only discusses studies that incorporate V2G charging. Alusio et al. [2] described an optimal day ahead operating strategy for microgrids with V2G EVs to minimize operating costs based on forecasted load demand and renewable generation. The authors used time-of-use energy rates for the analysis and demonstrated the optimization algorithm on a test microgrid. In Ref. 4, the authors carried out a techno-economic analysis of V2G in the Indonesian power grid considering 3 different tariffs: i) a fixed tariff which provided flat charging and discharging energy rates to EV owners, ii) a "natural" tariff which provided energy rates based on the electric generating resources, for example, geothermal, hydro, coal etc., iii) a demand response tariff which provided energy rates and incentives depending upon the amount of electricity supply and demand, i.e. the demand response tariff will increase when demand is high. The authors reported the environmental and economic advantages of incorporating V2G charging for both EV owners and utility companies. The authors in Ref. 5 presented an adjustable robust optimization scheduling model for a microgrid with renewable energy generation, V2G EVs, and time-of-use energy rates. Results showed improvements in the operational stability and economic performance of the microgrid, such as increasing the wind energy utilization, reducing peak-loads, and increasing minimum loads. Kiaee et al. [6] developed a

V2G simulator to undertake power flow analyses to compare the total charging cost of EVs with and without V2G technology within a power system consisting of 5,000 EVs using time-of-use energy rates. The control algorithm took advantage of arbitrage, while considering the EV capacity, the SOC, vehicle movement within the system and the requirements of drivers and power system operators. V2G charging achieved a 13.6% reduction in charging cost. A review paper [7] sheds light on various optimization algorithms used for EV scheduling for grid integration.

Schuller et al. [8] compared the weekly charging cost of EVs owned by different socio-economic groups by implementing V0G, V1G, and V2G charging strategies for residential charging with a time-of-use energy rate. Employees and retirees are the two socio-economic groups with the greatest contrast in driving behavior, driving 228 km and 119 km on average per week, respectively. For employees, weekly average costs are 32% and 45% less for V1G and V2G charging respectively as compared to V0G. For retirees, V1G and V2G charging saved about 51% and 62% respectively as compared to V0G. Datta et al. [9] proposed a charging/discharging strategy according to the price of electricity during off and on peak hours (i.e., time-of-use energy rates), and illustrated that the monthly cost savings associated with V2B is 11.6% as compared to V1G. Zhou et al. [10] optimized the provision of ancillary services to bring economic benefits to V2G EV owners in China under time-of-use energy rates. Refs. [11,12] further shed light on the capability of V2G EVs to shift charging from peak to off peak periods depending on time of use energy rates and demand response programs.

None of the studies discussed in the above literature review considered the effect of demand charges while optimizing V2G/V2B EV charge scheduling, even though demand charges are a significant portion (30 - 70%) of the electricity bill for commercial and industrial customers [13]. Very few studies directly deal with demand charges for EV charging [14]. Zhang et al. [14] proposed a V1G charging scheme for demand charge reductions, with the EV charging stations installed at four locations: large and small retail, recreation area, and workplace. The authors used real world Level 2 EV charging data for the analyses, where for the large retail (which is least flexible due to shorter charging events and higher EV mobility), 80% of the charging events were shorter than 3 hours. The proposed V1G smart charging scheme reduced monthly demand charges for large retail by 20-35% as compared to no-control charging for 30% EV demand penetration level, which is the percentage of EV energy demand with respect to the original (pre-EV) energy demand of the building. Refs. [15] and [16] considered demand charges for electric bus V1G fast charging stations but charging schedules of public buses differ from passenger EVs [15] with bus driving schedules being longer and rigid and energy requirements larger [15], and thus public bus charging is a unique problem [16]. Additionally, to the best of the authors' knowledge, only one previous work [8] presented a direct economic performance comparison of both V2G and V1G charging. Also, no previous work incorporated demand charges for commuter V2G/V2B EVs which the present work considers.

Although V2G/V2B scheduling strategies for economic cost optimization for time-of-use energy rates have been investigated previously, there are very few works on the long-term economic impact of smart charging. Most of the literature present case studies over a single day, week, or month to prove the efficacy of the schemes conceptually, as summarized in Table 1. However, at least year-long studies are needed to capture seasonal variations in building loads, EV demand, and tariffs.

Table 1. Simulation duration of other studies in literature

Work	Duration
Alusio et al. [2]	1 day
Shi et al. [5]	1 day

Zhou et al. [10]	1 day
Onishi et al. [11]	1 day
Zhang et al. [14]	1 day
Kiaee et al. [6]	5 weekdays
Schuller et al. [8]	7 days/1 week
Datta et al. [9]	30 days/1 month
Huda et al. [4]	1 year
Present Work	**1 year**
Li et al. [12]	10 years

1.3 Present work and its objective

In the present work, we analyze workplace V2B, V1G, and V0G charging with real load profiles from 14 commercial buildings, with 100% EV charging/discharging efficiency. The objective function minimizes the building electricity bill consisting of time-of-use energy and demand charges. One objective of this study is to report the optimal number of V2B charging stations to be installed at a particular building such that the original (pre-EV) operating electricity bill is not exceeded. The study also compares the electricity costs for 14 buildings under V0G, V1G and V2B charging strategies. Sensitivity analyses elucidate the effects of varying arrival and final state of charges (SOCs) on the total electricity bill. EV charging stations at commercial buildings are generally added "behind the meter" such that the energy consumed is lumped with the building energy consumption and adds to the commercial building owners' electricity costs. Commercial building owners typically either provide free charging to their employees or they contract with a third-party operator who collects charging fees from the EV owners. Charging fees can be structured such that charging (and discharging) flexibility is rewarded. Therefore, while the total electricity costs analyzed in this paper only directly apply to commercial building owners, some of the savings can be passed on to EV owners.

1.4 Novelty of the present work

The novelties of the present work are as follows:

- Realistic demand charges, which vary according to the time of the day and summer/winter season have been considered in the electricity bill. Ref. 14 considers demand charges whose rate varies according to the tier of demand (first 35 kW costs \$0/kW, next 115 kW costs \$5.72/kW and the remaining costs \$10.97/kW), but not according to time-of-day or season-wise. Ref. 14 also only considers V1G smart charging (no V2G/V2B analysis), and only for one EV demand penetration level (refer to Section 1.2).
- Two case studies are presented to quantify the electricity bill savings obtained by using V2G/V2B over V1G/V0G charging at commercial buildings: (A) A year-long case study, with variable number of EVs, using two daily EV layover intervals that are realistic, but uniform across the fleet; (B) A 5 day case study which is representative of a monthly analysis, based on historical EV charging data. Only Refs. 4 and 12 present studies with similar (or longer) time duration. Ref. 4 presents a year-long analysis of only V2G EV charging to show its effect on electricity cost reduction, but for a predefined fixed number (1 million) of V2G EVs. Ref. 12 presents a ten year analysis but also only considering V2G EVs. The motivation of Ref. 12 is also different, where V2G user and power grid company economic benefits (cost savings) are analyzed solely as a function of discharging power of the V2G EVs at the peaks (peak shaving load). Our study evaluates the electricity bill savings for commercial buildings

incorporating V2B charging as a function of number of EV charging stations, and additionally compares the V2B electricity costs to V1G and V0G charging electricity costs.

- The year-long analysis predicts the optimum number of V2B charging stations to be installed at a building, so as not to exceed the original (pre-EV) electricity bill.
- We derived and validated approximate analytical expressions for the total electricity costs as a function of EV charging demand. This is the first time that such equations have been derived. The equations allow for quick estimation of EV benefits worldwide.

The rest of the paper is organized as follows: Section 2 presents the problem formulation and discusses the optimization algorithm. Section 3 presents the results and discussion, and Section 4 presents the conclusions. Supplementary material is included at the end to present relevant discussion and results that expand upon the results presented in Section 3 of the main text. Any Section, Figure or Table referred to in this paper indicates to those in the main text unless specifically mentioned. References to the Supplementary material are explicitly mentioned wherever necessary.

2. Problem formulation and optimization algorithm

2.1 Overview of the fleet and charging scenarios

We aim to minimize the building electricity costs following the installation of a variable number of EV charging stations. To obtain representative savings, the analysis covers EV charging on all weekdays in 2019, while the weekend EV load is assumed to be zero. Weekends are excluded from EV charging as smaller building loads and less workplace charging preclude demand charge events, and time-of-use energy rate differences are smaller. Therefore, weekend EV charging does not materially impact the annual utility bill savings. Two case studies (A) and

(B) are considered. Case study (A), presented in part in the main text, and in part in Sections 1.1 through 1.2 of the Supplementary material, consists of an idealized uniform commuter fleet, where all EVs have the same battery, and arrive and depart daily at the same time, with the same initial and final SOC, respectively. The assumption of EVs arriving and departing at the same time daily is valid for certain type of buildings, such as hospitals and corporate buildings. Case study (A) is carried out for 14 commercial buildings located on the University of California (UC) San Diego campus, whose original load data can be found in Ref. 17. The buildings' primary functions are diverse and include classrooms, libraries, office spaces, and research laboratories. The load characteristics of the buildings for the analysis period (year 2019), along with their floor areas and year of construction are given in Table 2. Case study (B), presented completely in Section 3.5, considers a realistic case using historical EV charging data for a parking structure with 16 EV charging stations for 5 weekdays in February 2020, with the EV load being mapped to a building having 0 original load (the EV load thus becomes the net load of the building). The historical EV charging dataset contains the time of EV connection, disconnection and end of charging time, the amount of energy charged, the port type (Level 2 or Direct Current Fast Charger), and the initial and final SOC.

For V0G charging, the EVs charge at their maximum battery power, starting from the time the EVs are plugged in until meeting the charging energy demand, without any regard for the original building load. However, V1G and V2B EVs charge smartly to optimize the electricity costs, with V2B EVs having the additional capability to discharge back to the grid. Case studies (A) and (B) cover the application of the model for uniform EV fleet, and non-uniform realistic scenario based on historical EV charging data respectively, showing the efficacy of the optimization model in minimizing electricity costs for various scenarios.

Table 2. Mean original real load for all weekdays, mean of original monthly non-coincident demand peak and on-peak period demand peak (see definitions in Section 2.2), floor areas, number of floors, and year constructed of the buildings analyzed for the year 2019.

Building name (Building number)	Mean original real load (kW)	Mean original non-coincident demand peak (kW)	Mean original on-peak period demand peak (kW)	Building floor area (ft^2)	# of floors	Year Constructed
Mandeville Center (I)	32.2	60.1	56.9	131,365	4	1974
Police Department (II)	38.1	59.9	54.3	14,567	1	1991
Hopkins Parking Structure (III)	57.6	99.4	78.6	446,095	7	2006
Rady (Wells Fargo) Hall (IV)	60.3	103.1	98.8	93,440	4	2012
Pepper Canyon Hall (V)	62.0	102.4	91.5	85,985	4	2004
Otterson Hall (VI)	90.9	133.6	131.6	104,363	4	2007
Music Center (VII)	91.9	137.5	132.1	91,957	4	2008
Robinson Hall - 3 buildings (VIII)	95.0	134.7	129.9	32,932 + 5,142 + 29,618 = 67,724	4, 1, 2	1990
East Campus Office (IX)	118.3	156.4	146.4	77,164	3	2011
Center Hall (X)	122.8	194.4	186.2	83,288	4	1995
Student Services Center (XI)	140.5	242.9	202.1	135,085	4	2007
Social Sciences Building (XII)	146.5	200.0	184.5	84,386	5	1995
Galbraith Hall (XIII)	196.0	307.4	301.7	127,979	4	1965

Geisel Library (XIV)	532.0	649.2	644.0	416,509	10	1970

2.2 Objective function

The objective function to be minimized is the total electricity charges of the building plus a regularization term. The objective function is

$$\min[R_{\mathrm{NCDC}}(t) \times \mathrm{NCDP} + R_{\mathrm{OPDC}}(t) \times \mathrm{OPDP} + \{\sum_{d=1}^{d=m} \sum_{t=0}^{t=24\ \mathrm{h}-\Delta t} (R_{\mathrm{EC}}(t) \times \mathrm{NL}_{opt}(d,t) \times \Delta t)\} + \mathrm{OC}\ (d,t) + \mathrm{RT}\ (d,t)], \quad (1)$$

where R_{NCDC} is the non-coincident demand charge rate, NCDP is the non-coincident demand peak which is the maximum load demand from the grid at any 15 min interval of the month, R_{OPDC} is the on-peak demand charge rate, OPDP is the on-peak period demand peak which is the maximum load demand from the grid at any 15 min interval between 16:00 and 21:00 hours of all days of the month, $R_{\mathrm{EC}}(t)$ is the time-of-use energy charge rate, NL_{opt} is the building optimized net load demand from the grid, d is the index of the day of the month, m is the number of days of the month, t is the time of the day in hours, Δt is the time resolution which is chosen as 15 minutes (0.25 hours), consistent with the real load input data from the buildings, OC is other charges[1], and RT is a regularization term which guarantees a unique solution of Eq. (1). The first term in Eq. (1) is the non-coincident demand charge, the second term is the on-peak period demand charge, and the third term covers the off-peak and on-peak period energy costs over the entire month. The third term in Eq. (1) shows that for each day, the energy costs are covered from $t = 0$ to $t =$

[1] Other costs are the DWR Bond Charge (\$0.00580 × Total energy usage in a month), the City of San Diego Franchisee fee (\$0.0578 × $[\mathrm{R}_{\mathrm{NCDC}}(t) \times \mathrm{NCDP} + \mathrm{R}_{\mathrm{OPDC}}(t) \times \mathrm{OPDP} + \{\sum_{d=1}^{d=m} \sum_{t=0}^{t=24\ \mathrm{h}-\Delta t} (R_{\mathrm{EC}}(t) \times \mathrm{NL}_{opt}(d,t) \times \Delta t)\}]$), the DWR Bond franchisee fee ((\$0.0688 × DWR Bond Charge), the CA State Surcharge ((\$0.00030 × Total energy usage in a month), and the CA State Regulatory charge (\$0.00058 × Total energy usage in a month).

$24\text{ h} - \Delta t$. $t = 0$ corresponds to the time period from 00:00 to 00:15 hours, while $t = 24\text{ h} - \Delta t$ corresponds to the time period from 23:45 to 24:00 hours, thus covering the entire day. RT aims to minimize the deviation of the optimized net load from the original load (which indirectly avoids unnecessary charging/discharging cycles of the EV) as $\text{RT}\,(d,t) = wf \times \sum_{d=1}^{d=m} \sum_{t=0}^{t=24\text{ h}-\Delta t} \left\| \text{NL}_{opt}(d,t) - L_{org}(d,t) \right\|$, where $\|.\|$ is the 2-norm, wf is a weighting factor which is set as 0.01, and L_{org} is the original baseline building load.

2.3 Constraints

In this Section, for simplicity, d is dropped from the variable argument, with only t being retained, as the constraints are presented for one day. E.g., $\text{NL}_{opt}(d,t)$is written as $\text{NL}_{opt}(t)$. The daily power balance for each building is formulated as

$$\text{NL}_{opt}(t) = L_{org}(t) + \sum_{j=1}^{j=n} \text{EV}^j(t), \tag{2}$$

where n is the number of EVs, EV^j is the j^{th} electric vehicle charging rate where j is the EV index. Power flow from the grid to the EV (charging) is considered positive.

The EV charging rate is constrained as

$$\min \text{EV}^j \leq \text{EV}^j(t) \leq \max \text{EV}^j, \tag{3}$$

where the maximum and minimum EV charging rate depends upon the charging technology used (V0G/V1G/V2G/V2B). For V0G and V1G, $\min \text{EV}^j = 0$, whereas for V2G/V2B, $\min \text{EV}^j = -\max \text{EV}^j$.

The EV battery energy constraints are formulated as

$$\min \text{BE}^j \leq \text{BE}^j\,(t) \leq \max \text{BE}^j, \tag{4}$$

where BE^j is the Battery Energy of the j^{th} EV.

The minimum and maximum SOC of the battery are inputs, which in turn predefine the minimum and maximum battery energy limits.

The initial battery energy of the EV at the time of connection is formulated as

$$\mathrm{BE}^j\left(t = t_i^j\right) = \mathrm{SOC}_i^j \times \mathrm{BC}^j, \tag{5}$$

where SOC_i^j is the initial state of charge of the j^{th} EV, t_i^j is the time the j^{th} EV is connected to the charging station, "i" stands for "initial", and BC^j is the battery capacity of the j^{th} EV.

The battery energy variation with time is

$$\mathrm{BE}^j\,(t + \Delta t) = \mathrm{BE}^j\,(t) + \mathrm{EV}^j(t) \times \Delta t. \tag{6}$$

The total energy demand of the j^{th} EV (ED^j) is known beforehand as we use perfect forecasts. The final EV battery energy is constrained as

$$\mathrm{BE}^j\left(t = t_f^j\right) = \mathrm{BE}^j\left(t = t_i^j\right) + \mathrm{ED}^j, \tag{7}$$

where t_f^j is the disconnection time of the j^{th} EV, and "f" stands for "final". Furthermore, the total energy demand of the EV is formulated as

$$\mathrm{ED}^j = \left(\mathrm{SOC}_f^j - \mathrm{SOC}_i^j\right) \times \mathrm{BC}^j. \tag{8}$$

In case study (B), if Eq. (8), gives an infeasible energy demand (ED^j greater than the charging ability of the battery given the layover time), then the energy demand is corrected (ED_{cor}^j) as

$$\mathrm{ED}_{cor}^j = \min\left[\left(t_f^j - t_i^j\right) \times \max \mathrm{EV}^j, \mathrm{ED}^j\right], \tag{9}$$

where $\left(t_f^j - t_i^j\right)$ is the layover time.

Charging/discharging takes place within the layover period only and is constrained as

$$\mathrm{EV}^j(t) = 0 \qquad 0 \le t < t_i^j, \tag{10}$$

$$\mathrm{EV}^j(t) = 0 \qquad t_f^j < t \le t_{\mathrm{end}}^j, \tag{11}$$

where $t = 0$ and $t = t_{\mathrm{end}}^j$ correspond to the times at the start and end of the simulation.

2.4 Optimization software

The optimization is carried out in CVX, a package for specifying and solving convex programs [18,19] in the MATLAB environment. A flowchart for the optimization algorithm is shown in Fig. 1.

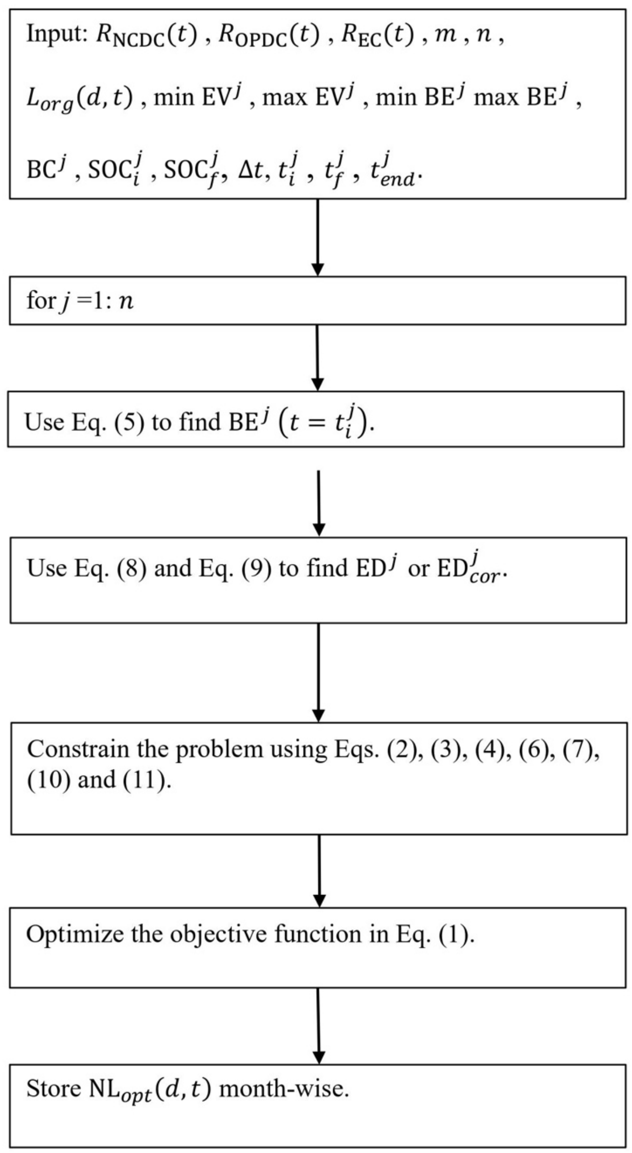

Figure 1. Flow chart of the optimization algorithm

2.5 Input Data for Case study (A) and (B)

Case study (A) is carried out for 14 metered UC San Diego buildings without EVs. The Case study (A) is further subdivided into two layover periods, a) 07:45 hours to 16:45 hours, which is representative of a typical office employee layover consisting of 8 hours of work-time, a 30 min lunch break and 30 mins for travel from the parking lot to the office and vice versa; and b) 06:30 hours to 19:30 hours, which is representative of a typical medical worker shift, consisting of 12 hours of work-time, a 30 min lunch break and 30 mins for travel from the parking lot to the medical center and vice versa. For Case study (A), the input variables that stay constant throughout the analysis are as follows. The battery capacity of all EVs (for j =1 through n) is chosen as $\mathrm{BC}^j = 60$ kWh which is representative of a typical EV [20]. The minimum and maximum SOC of the EVs are fixed at 20 and 90% respectively, to limit battery degradation during extreme charging states. The maximum charging rate of the EVs are $\max \mathrm{EV}^j$ =6.6 kW, which is a typical value for a Level 2 charger, which is the most prevalent type of EV charger in the United States [21]. For Case study (B), the minimum and maximum SOC of the EVs are fixed at 0 and 100% respectively, with variable EV battery capacity and initial & final SOCs per the real charging dataset. Furthermore, in case study (B), the maximum charging and discharging rate of the EVs depends on the type of EV charging port they are plugged into (Table 7). Case Study (B) uses real data from ChargePoint at UC San Diego, where the initial and final SOC is given for a subset of charging events. For these subsets of EV charging events, initial and final SOC varied between 0-100%. Thus, to impute the missing data consistent with the original data, the SOC range for Case study (B) is fixed between 0-100%.

The break-down of the electricity bill components levied by San Diego Gas & Electric are shown in Table 3. The non-coincident demand charge rates are constant throughout the year and are higher than the on-peak period demand charge rates in winter, but lower than the on-peak period demand charge rates in summer. The on-peak period energy charge rates are higher than the off-peak period energy charge rates throughout the year.

Table 3. Breakdown of electricity bill components - SDG&E AL-TOU tariff. The on-peak period is 16:00-21:00 hours, with the remaining hours being off-peak period hours. June 1 to October 31 are summer months with the rest of the year being winter.

Cost Component	Symbol	Value
Non-coincident demand charge rate (both summer and winter)	$R_{\mathrm{NCDC}}(t)$	\$24.48/kW
On-peak period demand charge rate (summer)	$R_{\mathrm{OPDC}}(t)$	\$28.92/kW
On-peak period demand charge rate (winter)		\$19.23/kW
Off-peak period energy charge rate (summer)	$R_{\mathrm{EC}}(t)$	\$0.10679/kWh
Off-peak period energy charge rate (winter)		\$0.09506/kWh
On-peak period energy charge rate (summer)		\$0.12628/kWh
On-peak period energy charge rate (winter)		\$0.10626/kWh

2.6 Input data for sensitivity analysis

A sensitivity analysis based on case study (A) is carried out to study the effect of varying the initial and final SOC of the EVs in Section 3.4. Initial and final SOC combinations of 40-80%, 45-85% and 50-90% are analyzed to study the effect of changing the initial and final SOCs while keeping the energy demand of the EVs constant. Energy demand sensitivity analyses are also carried out for initial and final SOC combinations of 50-85% and 50-80% to elucidate the effects of changing the final SOC while keeping the initial SOC constant.

3. Results and discussion

3.1 Idealized uniform commuter EV fleet case study

The results for building V (randomly selected) for initial and final EV SOC of 50% and 90% respectively for Jan (January) 2019 and the entire year 2019 are presented in Section 3.2 of the main text and Section 1.2 of the Supplementary material with graphics and summarized in Table 4. The $BC^j = 60$ kWh, and the initial and final SOC of 50 and 90% respectively correspond to a daily charging demand of 24 kWh per EV. Thus, the charging demand is increased in multiples of 24 kWh with each additional charging station / EV (see legend of figures in Section 3.2). The analyses are carried out up to 432 kWh charging demand (18 EV charging stations) as the changes in electricity costs per EV thereafter become independent of charging demand. The layover periods shown in the graphical analysis are 06:30 hours to 19:30 hours (Section 3.2) and 07:45 hours to 16:45 hours (Section 1.2 of the Supplementary material).

Figure 2 shows the original (pre-EV) load for building V for Jan 2019. The electricity load is low on holidays (Jan 1) and weekends (Jan 5, 6, 12, 13, 19, 20, 26, 27) when the building occupancy is low. The original non-coincident (NC) and on-peak period (PP) peak occur on Jan 31 at 14:00 hours at 109.0 kW and Jan 16 at 16:00 hours at 96.5 kW, respectively.

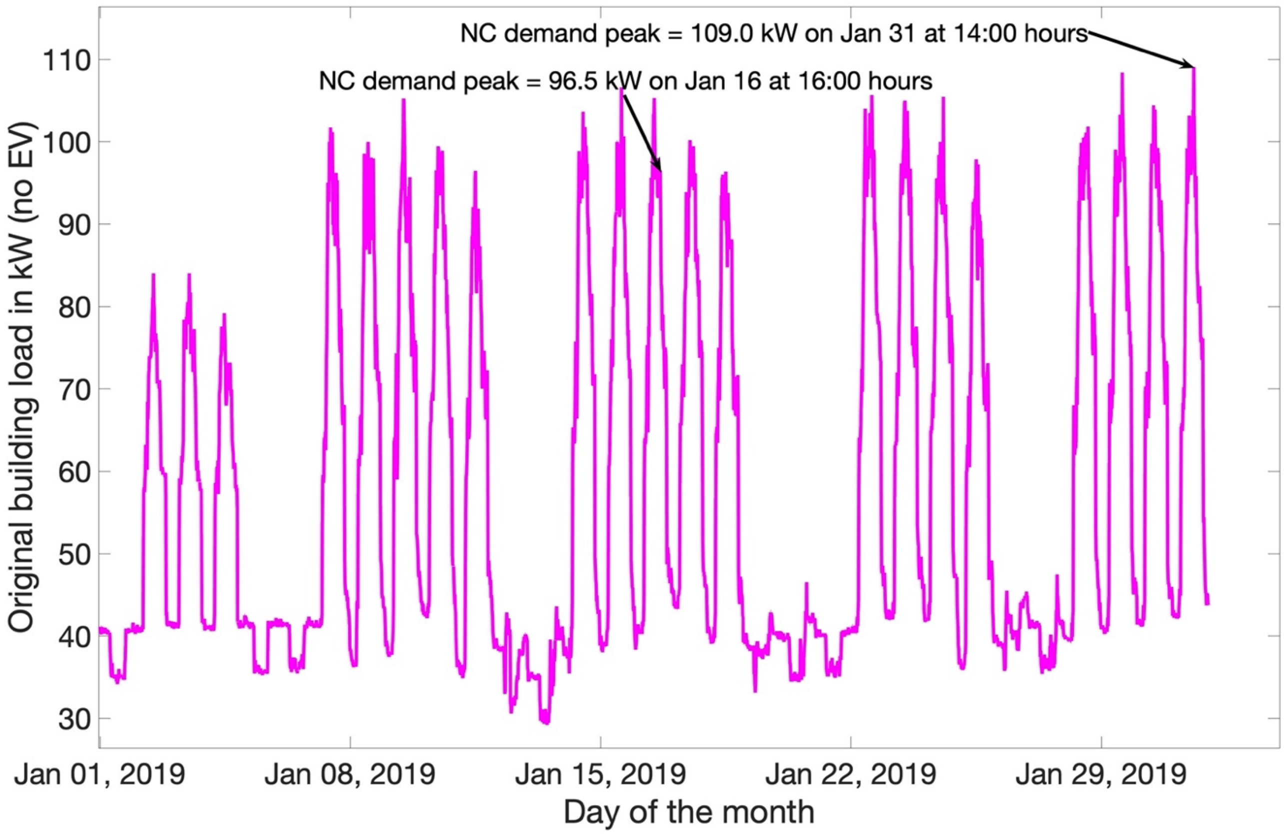

Figure 2. Original building V Load for Jan 2019

Table 4 shows the NC and PP demand peaks for Jan 2019 for building V for selected EV charging demand scenarios for both layover periods.

Table 4. Summary of the NC and PP demand peaks for all charging strategies for Jan 2019 for building V. The original NC and PP demand peaks are 109.0 and 96.5 kW respectively. The peak values (with EV charging) which are larger / smaller than the original are marked in red / green font.

Daily EV charging demand	Layover 06:30-19:30 hours		Layover 07:45-16:45 hours	
	NC demand peak (kW)	PP demand peak (kW)	NC demand peak (kW)	PP demand peak (kW)

(kWh) (# of EVs/ charging stations)	V0G	V1G	V2B	V0G	V1G	V2B	V0G	V1G	V2B	V0G	V1G	V2B
24 (1)	110.6	109.0	102.4	96.5	96.5	89.9	111.0	109.0	102.4	96.5	96.5	91.0
48 (2)	117.2	109.0	99.5	96.5	96.5	83.5	117.6	109.0	102.6	96.5	96.5	91.0
72 (3)	123.8	109.0	101.5	96.5	96.5	82.4	124.2	109.0	105.0	96.5	96.5	91.0
96 (4)	130.4	109.0	103.1	96.5	96.5	82.4	130.8	109.0	107.6	96.5	96.5	91.0
120 (5)	137.0	109.0	105.0	96.5	96.5	82.4	137.4	109.8	110.3	96.5	96.5	91.0
144 (6)	143.6	109.0	107.1	96.5	96.5	82.4	144.0	112.7	113.2	96.5	96.5	91.0
168 (7)	150.2	109.0	109.6	96.5	96.5	82.4	150.6	115.6	116.1	96.5	96.5	91.0
192 (8)	156.8	109.0	112.1	96.5	96.5	82.4	157.2	118.5	119.0	96.5	96.5	91.0
216 (9)	163.4	109.5	114.7	96.5	96.5	82.4	163.8	121.4	121.9	96.5	96.5	91.0
240 (10)	170.0	112.0	117.2	96.5	96.5	82.4	170.4	124.3	124.8	96.5	96.5	91.0
432 (18)	222.8	132.2	137.4	96.5	96.5	82.4	223.2	147.6	148.1	96.5	96.5	91.0

3.2 Layover 06:30 hours to 19:30 hours- medical worker shift

3.2.1 V0G charging

The V0G EVs start charging the moment they are plugged in (06:30 hours) at the highest possible EV battery power rate (6.6 kW), resulting in charging terminating by 10:15 hours. The highest original load in the 06:30-10:15 hours period occurs on Jan 22 at 09:30 hours and is 104.0 kW. Therefore, on Jan 22 the net load (with V0G EVs) at 09:30 hours for 24 kWh (1 EV) of charging demand, which contributes 6.6 kW of charging load, becomes the V0G NC monthly demand peak at 110.6 kW (see Table 4). The V0G monthly demand peak increases with further increasing charging demand by 6.6 kW per EV. As all charging occurs before the on-peak period, the PP demand peak remains the same as the original at 96.5 kW. Refer to Figure 1 of the Supplementary material for a graphical representation**.**

3.2.2 V1G charging

V1G chargers cannot discharge back into the grid, and hence the optimized net load (with EV charging) cannot be smaller than the original load. Figure 3(a) shows that on Jan 31, with up to 192 kWh of charging demand, the NC demand peak remains the same as the original at 109.0 kW. Increasing the charging demand to 216 kWh increases the NC demand peak to 109.5 kW, which exceeds the original NC demand peak. With the addition of more V1G EV charging demand (above 216 kWh charging demand), the optimal NC peak demand increases by 2.5 kW per EV because the increasing charging demand (of 24 kWh per EV) is uniformly spread out over the 9.5 hour off-peak layover period from 06:30-16:00 hours (see Section 3.2.4 for a detailed explanation).

Figure 3(b) shows that the PP demand peak remains the same as the original at 96.5 kW for all charging demands. Because of the higher energy and demand charges applicable in the on-peak period as compared to the off-peak period, all charging will take place in the off-peak layover period before 16:00 hours if feasible. A complete charging before 16:00 hours occur on some days (e.g. Figure 3(b) for 1 or 2 EVs) when accommodating all the charging demand within the off-peak layover period does not lead to an increase of the NC demand peak beyond the original. However, complete charging before 16:00 hours is not optimal on days when the original off-peak load curve during the layover period cannot accommodate the charging demand without increasing the NC demand peak. Therefore, charging during the off-peak layover period (from 06:30-16:00 hours) takes place until the optimized load becomes constant at the original NC demand peak. A further increase in the charging demand results in EVs being charged during the on-peak layover period (16:00-19:30 hours) until the optimized on-peak layover period load becomes constant at the original PP demand peak. With further increasing the charging demand, charging occurs again exclusively in the off-peak layover period (06:30-16:00 hours), leading to increasing NC demand peak beyond the original demand peak (see Fig. 3(c)). Specifically, the additional charging demand is spread out uniformly over the off-peak layover period. The reasoning for the optimized charging strategy is given in Section 3.2.4.[2]

Figure 3(c) shows the V1G timeseries analysis on Jan 22 to elucidate the optimized charging strategy. For a charging demand of 24 kWh, the entire charging takes place in the off-peak layover period. With further increasing charging demand (192 kWh), charging continues to occur in the off-peak layover period until the off-peak layover period load becomes constant at the original NC demand peak (109.0 kW), with the rest of the charging occurring in the on-peak period without increasing the PP demand peak (96.5 kW). For a charging demand of 216 kWh, additional charging occurs initially in the on-peak period until the on-peak layover period load becomes constant at the PP demand peak, with the rest of the additional charging demand being uniformly accommodated in the off-peak layover period increasing the NC demand peak to 109.5 kW. With further increasing charging demand (above 216 kWh), additional charging occurs exclusively in the off-peak layover period, with the additional charging demand spread out uniformly, leading to an increase in the NC demand peak by 2.5 kW per EV (see Table 4). Comparing Figs. 3(a) and 3(c) show that for some charging demands, the optimized NC and PP demand peaks are reached on multiple days.

[2] Note that in rare cases the maximum EV charging rate can restrict the maximum charging such that charging deviates slightly from the strategy described above. But most of the results relevant to this paper can be explained by the optimized charging strategy discussed above.

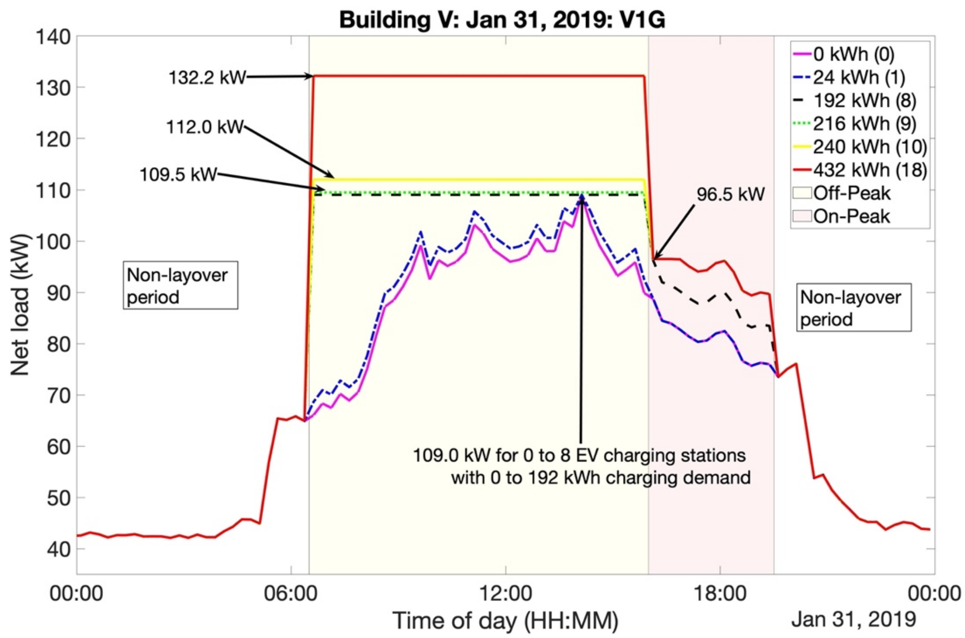

Building V: Jan 31, 2019: V1G
Net load (kW)
Time of day (HH:MM)
Jan 31, 2019
132.2 kW
112.0 kW
109.5 kW
96.5 kW
109.0 kW for 0 to 8 EV charging stations
with 0 to 192 kWh charging demand
Non-layover period
Non-layover period
0 kWh (0)
24 kWh (1)
192 kWh (8)
216 kWh (9)
240 kWh (10)
432 kWh (18)
Off-Peak
On-Peak

(a)

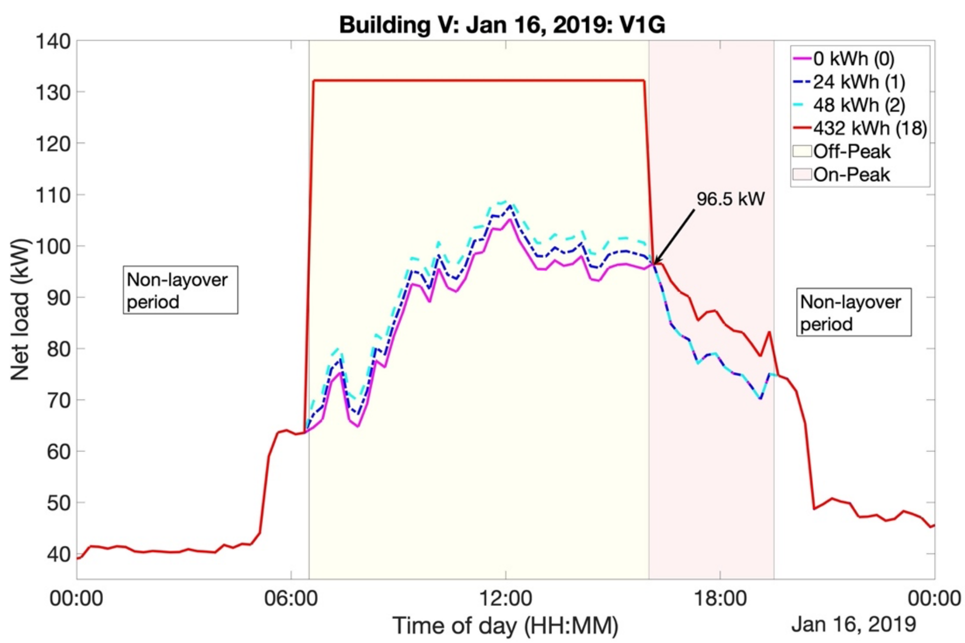

Building V: Jan 16, 2019: V1G
Net load (kW)
Time of day (HH:MM)
Jan 16, 2019
96.5 kW
Non-layover period
Non-layover period
0 kWh (0)
24 kWh (1)
48 kWh (2)
432 kWh (18)
Off-Peak
On-Peak

(b)

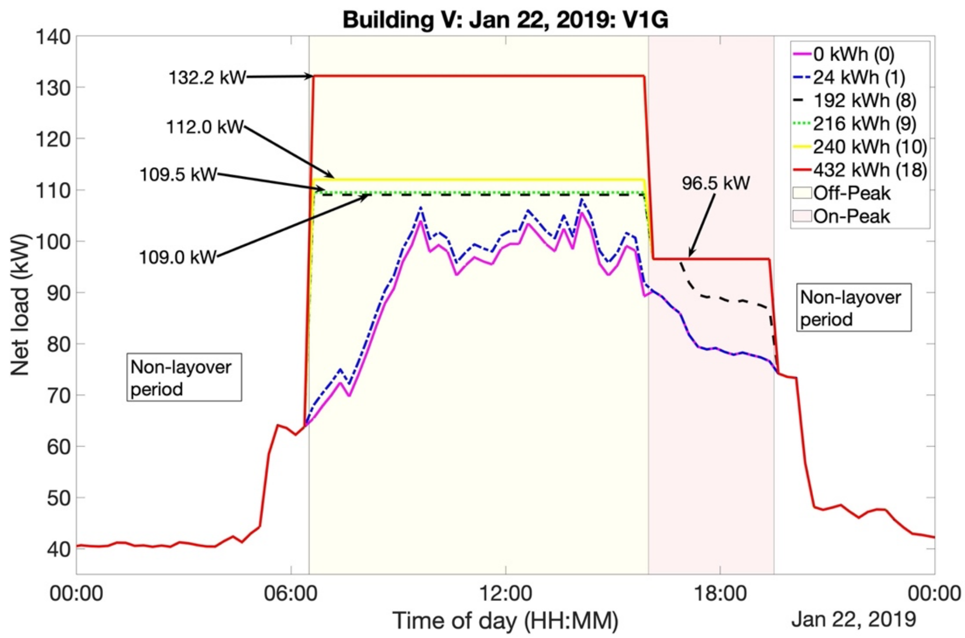

(c)

Figure 3. V1G charging for the 06:30-19:30 hours layover: (a) NC demand peak for Jan 31 2019, when the original NC demand peak also occurs, (b) PP demand peak for Jan 16 2019, when the original PP demand peak also occurs, and (c) NC and PP demand peak for Jan 22 2019, which provides the greatest limitation for accommodating PP EV charging. The legend shows total daily EV charging demand and the number in brackets in the legend correspond to the number of EVs/charging stations. The yellow shading denotes the off-peak layover period, the red shading denotes the on-peak layover period, while the un-shaded area denotes the non-layover period. The original NC and PP demand peaks are 109.0 and 96.5 kW, respectively.

3.2.3 V2B charging

Figure 4(a) shows that the V2B chargers can discharge and decrease the optimized net load below the original load. For example, the NC demand peak decreases from 109.0 kW to 102.4 kW and then to 99.5 kW as the charging demand increases from 0 kWh to 24 kWh and then to 48 kWh respectively. This occurs because as the number of EVs increases, the total discharge power also increases. However, from a charging demand of 72 kWh, we see a monotonous increase in the NC demand peak, and starting at 168 kWh the optimized NC demand peak exceeds the original NC demand peak. Above a charging demand of 168 kWh, the NC demand peak increases by 2.5 kW per EV (see Table 4), as the additional charging demand (over 168 kWh) is spread out uniformly over the entire off-peak layover period. The reasoning for this optimized V2B charging strategy is elucidated in Section 3.2.4. The variation in the optimized net load around 07:00 hours for all energy demands in Fig. 4(a) occurs due to the regularization term in the objective function that penalizes the deviation from the original load curve. The optimized load is equal to the NC demand peak after about 10:00 hours since no extra cost is incurred when the optimized load is equal to the NC demand peak threshold. A detailed discussion is provided in Section 1.1.2 of the Supplementary material.

Figure 4(b) shows the on-peak period on Jan 16 which is the day with the original PP peak. With increasing charging demand from 24 kWh to 72 kWh, the PP demand peak decreases. The increased discharging capacity with the addition of more EVs is responsible for the reduction of the PP demand peak. With further increasing charging demand, the PP demand peak remains constant at 82.4 kW. The NC and PP demand thresholds for Jan are decided by different days depending on charging demand. Jan 16 decides the demand thresholds for 1 EV (for 24 kWh daily charging demand). Then, Jan 22 (shown graphically in Fig. 2 of Supplementary material) decides the demand thresholds for 2 or more EVs as shown by flat lines at 83.5 kW (2 EVs, 48 kWh) and 82.4 kW (3 or more EVs, 72 kWh or more).

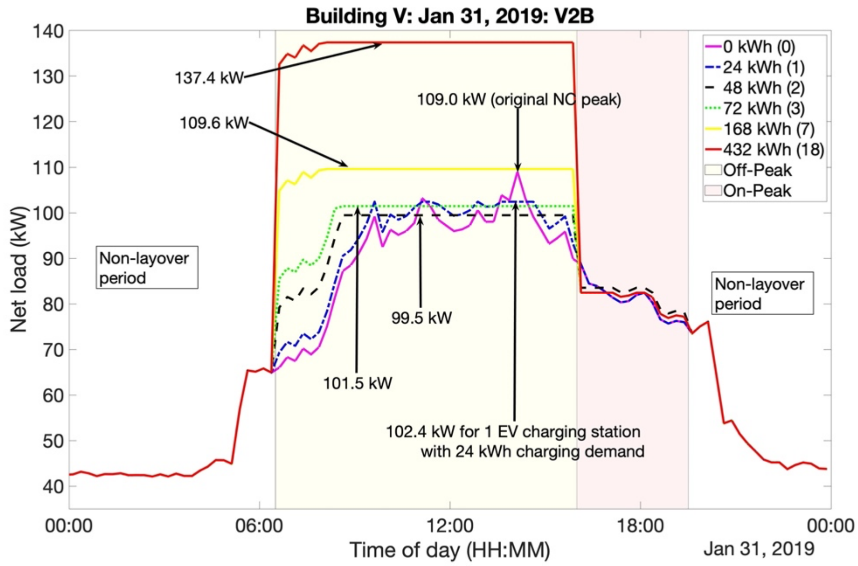

(a)

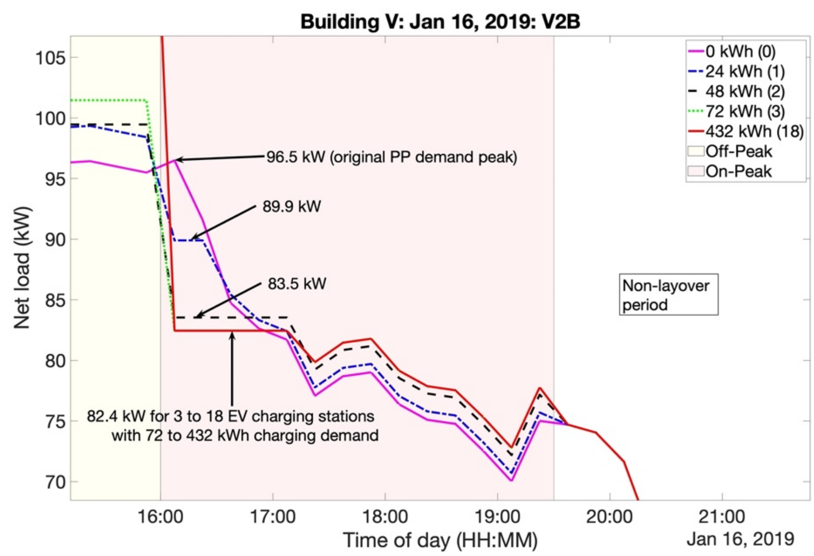

(b)

Figure 4. V2B charging for the 06:30-19:30 hours layover: (a) NC demand peak for Jan 31, 2019, when the original NC demand peak also occurs, and (b) PP demand peak for Jan 16, 2019 when the original PP demand peak also occurs. The original NC and PP demand peaks are 109.0 and 96.5 kW, respectively.

3.2.4 Effect of charging type, load shape and layover period on electricity costs

3.2.4.1 Cumulative results: 06:30-19:30 hours layover

Section 3.2.1 through 3.2.3 elucidate the effect of the charging demand (or number of charging stations) on the NC and PP demand peaks for Jan 2019 for the layover period 06:30-19:30 hours. In Section 3.2.4, we compare the performance between V0G, V1G and V2B charging strategies in terms of total electricity costs for Jan and the entire year 2019 for the layover period 06:30-19:30 hours. We also derive general mathematical expressions for the slopes (once they become constant) of the V0G, V1G and V2B total electricity charges versus daily energy demand curves month-wise, daily charging demand when the V1G and V2B curves transition to constant slope, and final offset between V1G and V2B total electricity charges. Although, we mostly present results from building V in this paper, the mathematical expressions are applicable to all the other buildings and for other layover periods.

Figures 5 shows that for both Jan (Fig. 5a) and the entire year 2019 (Fig. 5b), the total electricity costs with V2B are lower than the original building costs for charging capacities up to 120 kWh (or 5 V2B charging stations), making 5 the optimal number of V2B charging station installations for building V for the layover period 06:30-19:30 hours.

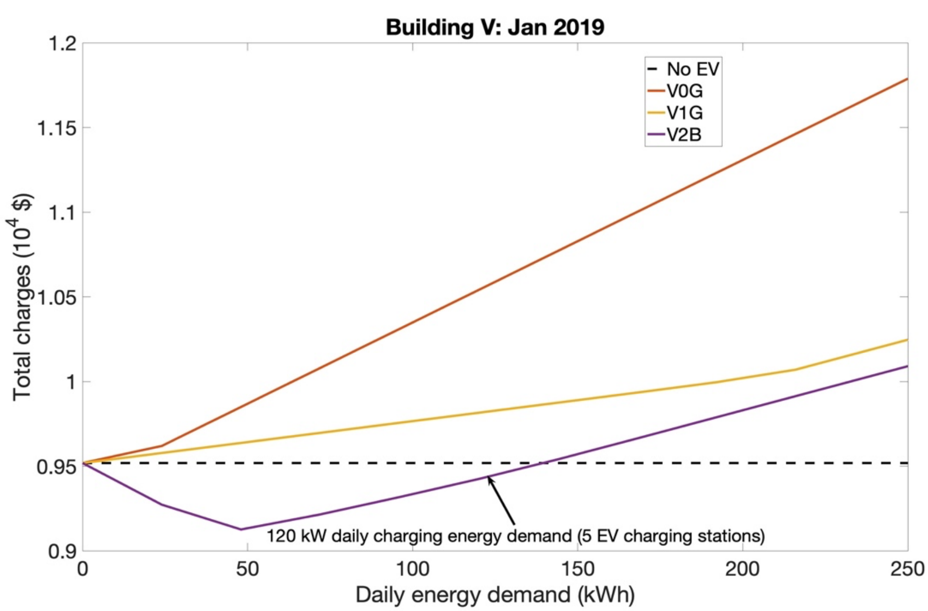

(a)

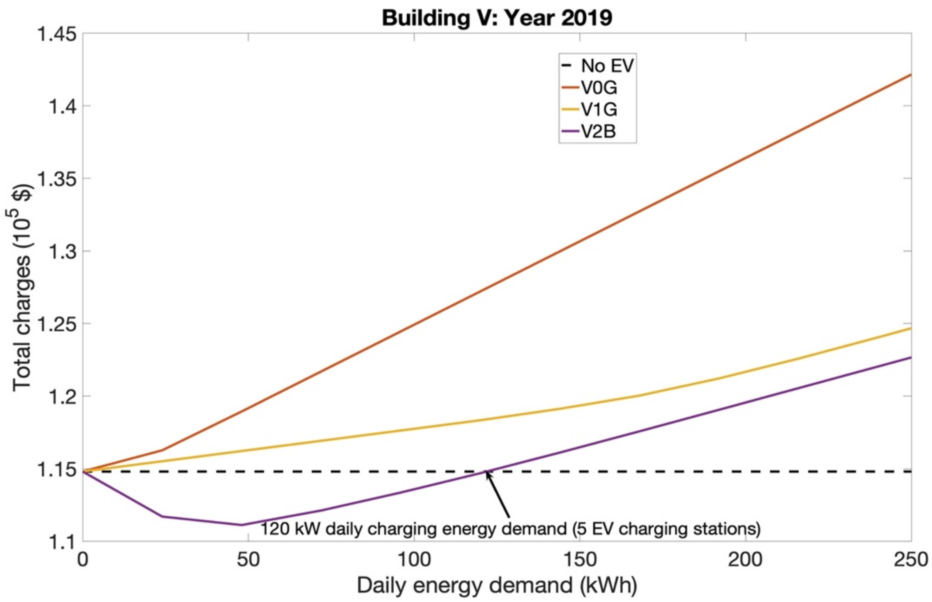

(b)

Figure 5. Total electricity charges versus total daily EV energy demand for (a) Jan 2019 and (b) the entire year 2019 for the layover period 06:30-19:30 hours at building V.

Figures 5 also shows that V0G charging incurs the highest electricity costs, followed by V1G and V2B respectively. This is expected as V0G cannot time-shift load demand from the grid and charges at the maximum charger power of 6.6 kW, while for V1G and V2B, charging is spread out smartly to optimize electricity costs. V2B reduces the electricity costs compared to V1G because the V2B discharging capability reduces the demand peak costs. The net summation of NC and PP demand peak charges are less for V2B than V1G which results from a greater reduction in PP demand peak charges compared to the increase in NC demand charges (Table 4). The net cost savings as a result of shifting demand from the on-peak to off-peak layover period of V2G/V2B EVs are demonstrated for a hypothetical case study in Section 1.3 of the Supplementary material.

Initially the V2B and V1G electricity costs diverge because with an increasing number of EVs, the V2B EVs can discharge during the non-coincident and on-peak period peaks, while charging at other times, which leads to reduced costs. However, after a certain energy demand, Figs. 5(a) and 5(b) show that the V1G and V2B cost curves become parallel to each other.

For V1G, as described in Section 3.2.2, after both the off-peak and on-peak layover period loads become constant (at their respective original peaks), additional charging demand is accommodated in the off-peak layover period only. Accommodating the additional charging demand exclusively in the off-peak layover period leads to an increase of the non-coincident demand peak as, $\Delta\mathrm{NCDP} = \frac{\Delta\mathrm{CD_{day}}}{16\ \mathrm{h} - t_i^j}$, where $\Delta\mathrm{NCDP}$ is the increase of the NC demand peak, $\Delta\mathrm{CD_{day}}$ is the daily increase in the charging demand and $(16\ \mathrm{h} - t_i^j)$ is the off-peak layover which is 9.5 hours (06:30-16:00 hours) for the 06:30-19:30 hours layover. Accommodating the daily increase in charging demand exclusively in the on-peak layover period would increase the on-peak period demand peak as, $\Delta\mathrm{OPDP} = \frac{\Delta\mathrm{CD_{day}}}{t_f^j - 16\ \mathrm{h}}$, where $\Delta\mathrm{OPDP}$ is the increase of the PP demand peak and $(t_f^j - 16\ \mathrm{h})$ is the on-peak layover which is 3.5 hours (16:00-19:30 hours) for the 06:30-19:30 hours layover. Therefore, after the net loads are flat, V1G charging only occurs in the off-peak layover period if $\Delta\mathrm{NCDP} \times R_{\mathrm{NCDC}}(t) - \Delta\mathrm{OPDP} \times R_{\mathrm{OPDC}}(t) < 0$, which is the case as $\frac{\mathrm{R_{NCDC}(t)}}{\mathrm{R_{OPDC}(t)}} < \frac{16\ \mathrm{h} - \mathrm{t_i^j}}{\mathrm{t_f^j} \text{-} 16\ \mathrm{h}}$ for both summer and winter. Table 3 shows that the ratio of $R_{\mathrm{NCDC}}(t)$ to $R_{\mathrm{OPDC}}(t)$ is 1.27 for winter and 0.85 for summer. For the 06:30-19:30 hours layover, the ratio of off-peak (9.5 hours) to on-peak (3.5 hours) layover duration is 2.7. Table 3 also shows that the PP energy charges are higher than the off-peak period energy charges for both summer and winter. Thus, after the net loads are flat, accommodating the additional charging demand uniformly in the off-peak layover period is most economical from both the energy and demand charges point of view.

For V2B, with a small charging demand it is economical to discharge during the off and on-peak period peaks, and charge at other times such that the off and on-peak layover period loads become constant, since a constant net load by definition has the smallest peak. The divergence of V2B and V1G electricity costs for a small number of EVs occurs as the V2B EVs – unlike V1G - can discharge during the original off-peak and on-peak period peaks, reducing the NC and PP demand peaks. With further increasing charging demand, once the off peak and on peak period loads are constant, it is most economical to spread out the additional charging demand exclusively over the off-peak layover period, keeping the PP load constant (as shown in Fig. 2 in supplementary material above 168 kWh charging demand) for the same reason discussed above for V1G charging. When additional charging demand is accommodated by charging in the off-peak layover period only, V2B offers no further economic advantages over V1G. If the V2B EVs were to discharge at a given time, the same amount of energy would have to be charged at another time and therefore introduce a new peak. Thus, the V1G and V2B electricity costs become parallel after a certain energy demand as the additional energy and demand cost per added vehicle is identical. The trends of the total electricity charges versus the total daily EV energy demand curve for electricity tariff structures other than those in this paper are similar to Fig. 5 as discussed in Section 1.4 of the Supplementary material.

3.2.4.2 Final slope of total electricity charges versus daily EV charging demand curve

For V0G charging in Jan 2019 and daily charging/energy demand over 24 kWh (see Table 4), when the slope of the V0G total electricity charges versus charging demand curve becomes constant (see Fig, 5(a)), with every 24 kWh of daily additional EV charging demand ($\Delta \mathrm{CD}_{\mathrm{day}}$), the ΔNCDP is 6.6 kW while the ΔOPDP is 0, which leads to an increase in the NCDC as $\Delta \mathrm{NCDC} = \Delta \mathrm{NCDP} \times R_{\mathrm{NCDC}}(t)$, where $R_{\mathrm{NCDC}}(t)$ is \$24.48/kW. The total charging demand increase in the month is $\Delta\mathrm{CD}_{\mathrm{month}} = \Delta\mathrm{CD}_{\mathrm{day}} \times \mathrm{Weekdays}$, where $\mathrm{Weekdays} = 23$ for Jan 2019. The entire charging demand is added in the off-peak layover period which leads to increasing monthly energy charges as $\Delta\mathrm{EC}_{\mathrm{month}} = \Delta\mathrm{CD}_{\mathrm{month}} \times R_{\mathrm{EC}}(t)$, where $R_{\mathrm{EC}}(t)$ is \$0.09506/kWh. Due to the increase in NCDC and energy charges, there is a corresponding increase in other charges as $\Delta\mathrm{OC} = [0.00580 + 0.00030 + 0.00058 + (0.0688 \times 0.00580)] \times \Delta\mathrm{CD}_{\mathrm{month}} + 0.0578 \times (\Delta\mathrm{NCDC} + \Delta\mathrm{EC}_{\mathrm{month}})$.

For the V1G and V2B charging, when the final slopes of their total electricity charges versus daily energy demand curves become constant for a month, further increasing daily charging demand ($\Delta\mathrm{CD}_{\mathrm{day}}$) is accommodated and spread out uniformly over the off-peak layover period. This leads to $\Delta\mathrm{NCDP} = \frac{\Delta\mathrm{CD}_{\mathrm{day}}}{16\ \mathrm{h} - t_i^j}$, while the equations governing $\Delta\mathrm{NCDC}$, $\Delta\mathrm{CD}_{\mathrm{month}}$, $\Delta\mathrm{EC}_{\mathrm{month}}$ and $\Delta\mathrm{OC}$ remain the same as those of V0G. The final slope of the V0G, V1G and V2B total electricity charges versus energy daily demand curves, once they become constant for the month, is governed by

$$\mathrm{Slope}_{\frac{\mathrm{V0G}}{\frac{\mathrm{V1G}}{\mathrm{V2B}}}} = \frac{\Delta\mathrm{NCDC} + \Delta\mathrm{EC}_{\mathrm{month}} + \Delta\mathrm{OC}}{\Delta\mathrm{CD}_{\mathrm{day}}}, \quad (12)$$

where the difference between the slopes of V0G and V1G/V2B, once they become constant, is determined by $\Delta\mathrm{NCDP}$ (and hence $\Delta\mathrm{NCDC}$), which are different for V0G and V1G/V2B charging.

3.2.4.3 Daily EV charging demand when the V1G and V2B total electricity charges versus daily EV charging demand curve transitions to constant slope

The daily V1G charging demand above which the final slope of the total electricity charges versus daily energy demand becomes constant for a month is approximated by calculating the V1G threshold daily charging demand ($\mathrm{CD}_{\mathrm{day,thr,V1G}}$) above which charging takes place in the off-peak layover period only.

For any weekday of the month, for daily charging demands ($\mathrm{CD}_{\mathrm{day}}$) for (and above) which V1G charging takes place in the off-peak layover period only satisfies

$$\mathrm{ED}_{org}(d) + \mathrm{CD}_{\mathrm{day}} \geq \mathrm{NCDP}_{org} \times (16\mathrm{h} - t_i^j) + \mathrm{OPDP}_{org} \times \left(t_f^j - 16\mathrm{h}\right), \quad (13a)$$

where NCDP_{org} and OPDP_{org} are the original NCDP and OPDP, respectively. Furthermore, $\mathrm{ED}_{org}(d)$ is the original energy demand during the EV layover period on "d" day of the month, formulated as $\mathrm{ED}_{org}(d) = \sum_{t_i^j}^{t_f^j}(L_{org}(d,t) \times \Delta t)$.

The V1G threshold daily charging demand is calculated by using an equality operator in Eq. (13a), for the day of the month when the original energy demand for the day during the layover period is maximum, and is formulated as

$$\mathrm{CD}_{\mathrm{day,thr,V1G}} = \mathrm{NCDP}_{org} \times \left(16\mathrm{h} - t_i^j\right) + \mathrm{OPDP}_{org} \times \left(t_f^j - 16h\right) - \max \mathrm{ED}_{org}, \quad (13b)$$

where $\max \mathrm{ED}_{org}$ is the maximum of $\mathrm{ED}_{org}(d)$ of all weekdays of the month.

If there are no limitations on the optimized charging due to maximum power constraints (as is the case for the 06:30-19:30 hours EV layover at building V, discussed in Section 3.2.2), Eq. (13b) accurately predicts the daily V1G charging demand above which the final slope of the total electricity charges versus daily energy demand becomes constant. Otherwise, Eq. (13b) yields a lower bound.

Ideally, the V2B EVs would discharge at their maximum power back to the grid at the original NC and PP demand peak times resulting in the off-peak and on-peak period loads becoming constant at the reduced off-peak and on-peak demand peaks. After that, charging should take place in the off-peak layover period only. The V2B threshold daily charging demand ($\mathrm{CD}_{\mathrm{day,thr,V2B}}$) above which charging takes place in the off-peak layover period only is approximated as

$$\mathrm{CD_{day,thr,V2B}} = [\mathrm{NCDP}_{org} - \max \mathrm{EV}^j \times p] \times \left(16\mathrm{h} - t_i^j\right) + [\mathrm{OPDP}_{org} - \max \mathrm{EV}^j \times p] \times \left(t_f^j - 16\mathrm{h}\right) - \max \mathrm{ED}_{org}, \tag{14a}$$

where p is the number of EVs corresponding to $\mathrm{CD_{day,thr,V2B}}$.

$$p = \frac{\mathrm{CD_{day,thr,V2B}}}{\mathrm{CD_{EV}}}, \tag{14b}$$

where $\mathrm{CD_{EV}}$ is the daily charging demand of one EV.

Combining Eqs. (14a) and (14b), we get

$$\mathrm{CD_{day,thr,V2B}} = \frac{\mathrm{NCDP}_{org} \times \left(16\mathrm{h} - t_i^j\right) + \mathrm{OPDP}_{org} \times \left(t_f^j - 16h\right) - \max \mathrm{ED}_{org}}{1 + \frac{\max \mathrm{EV}^j \times \left(16\mathrm{h} - t_i^j\right)}{\mathrm{CD_{EV}}} + \frac{\max \mathrm{EV}^j \times \left(t_f^j - 16\mathrm{h}\right)}{\mathrm{CD_{EV}}}}. \tag{14c}$$

$\mathrm{CD_{day,thr,V2B}}$ is a lower bound for the daily V2B charging demand above which the final slope of the total electricity charges versus daily energy demand becomes constant. This is because V2B EVs do not discharge at the maximum power at the original NC and PP demand peak times as Eq. (14c) does not take into account if the EV charging demand is met or not at the time of the EV departure.

$\mathrm{CD_{day,thr,V2B}} \leq \mathrm{CD_{day,thr,V1G}}$ because of V2B EV's ability to discharge (V1G is the limiting worst case of V2B). Thus, the threshold daily charging demand above which charging takes place in the off-peak layover period only for both V1G and V2B is decided by $\mathrm{CD_{day,thr,V1G}}$ calculated from Eq. (13b).

3.2.4.4 Final monthly offset between the V1G and V2B total electricity charges

The final monthly offset between V1G and V2B (the difference between the V1G and V2B total electricity charges) once the final slopes of both V1G and V2B total electricity charges versus daily energy demand curves become constant can be approximated for any $\mathrm{CD_{day}} \geq \mathrm{CD_{day,thr,V1G}}$.

Choosing a $\mathrm{CD_{day}}$ corresponding to p number of EVs where $\mathrm{CD_{day}} \geq \mathrm{CD_{day,thr,V1G}}$, the final monthly offset between V1G and V2B is

$$\mathrm{Offset} = R_{\mathrm{NCDC}}(t) \times (\mathrm{NCDP_{V1G}} - \mathrm{NCDP_{V2B}}) + R_{\mathrm{OPDC}}(t) \times (\mathrm{OPDP_{V1G}} - \mathrm{OPDP_{V2B}}) + \{\textstyle\sum_{\mathrm{Weekdays}}(\mathrm{EC_{day,V1G}} - \mathrm{EC_{day,V2B}})\} + (\mathrm{OC_{V1G}} - \mathrm{OC_{V2B}}), \tag{15}$$

where the energy charges (EC) and the OC are calculated for the EV layover period times on weekdays only. Outside the EV layover times, the electricity charges for V1G and V2B are identical and equal to the original electricity charges.

For V1G charging, for the $\mathrm{CD_{day}}$ above which charging takes place in the off-peak layover period only, $\mathrm{OPDP_{V1G}}$ is

$$\mathrm{OPDP_{V1G}} = \mathrm{OPDP_{org}}. \tag{16a}$$

$\mathrm{NCDP_{V1G}}$ is calculated based on the day of the month when the original energy demand during the layover period is maximum, and is formulated as

$$\mathrm{NCDP_{V1G}} = \frac{\left[\max \mathrm{ED}_{org} + \mathrm{CD_{day}} - \mathrm{OPDP_{V1G}} \times \left(t_f^j - 16\mathrm{h}\right)\right]}{\left(16\ \mathrm{h} - t_i^j\right)} \tag{16b}$$

$$\mathrm{EC_{day,V1G}} = \mathrm{EC_{day,V1G.off}} + \mathrm{EC_{day,V1G,on}}, \tag{16c}$$

where $\mathrm{EC_{day,V1G}}$, $\mathrm{EC_{day,off,V1G}}$, and $\mathrm{EC_{day,on,V1G}}$ are the daily V1G total, off-peak, and on-peak layover energy charges, respectively. For one weekday, $\mathrm{EC_{day,off,V1G}}$ and $\mathrm{EC_{day,on,V1G}}$ is approximated as

$$\mathrm{EC_{day,off,V1G}} = \textstyle\sum_{t_i^j}^{16\ \mathrm{h}} \min\left[(L_{org}(t) + \max \mathrm{EV}^j \times p), \mathrm{NCDP_{V1G}}\right] \times R_{\mathrm{EC}}(t) \times \Delta t. \tag{16d}$$

$$\mathrm{EC_{day,on,V1G}} = \{(\textstyle\sum_{t_i^j}^{t_f^j} L_{org}(t)) + \frac{\mathrm{CD_{day}}}{\Delta t} - \textstyle\sum_{t_i^j}^{16\ \mathrm{h}} \min\left[(L_{org}(t) + \max \mathrm{EV}^j \times p), \mathrm{NCDP_{V1G}}\right]\} \times R_{\mathrm{EC}}(t) \times \Delta t. \tag{16e}$$

For V2B charging, on the day which determines the $\mathrm{OPDP_{V2B}}$, the EVs charge to their maximum SOC during the off-peak layover to have maximum discharging capability during the on-peak layover. The on-peak layover energy demand (ED_{on}) on the day which determines the $\mathrm{OPDP_{V2B}}$ is formulated as

$$\mathrm{ED}_{on} = \{\mathrm{BE}^{j}\left(t = t_f^j\right) - \max \mathrm{BE}^{j}\} \times p\,. \tag{17a}$$

The $\mathrm{OPDP_{V2B}}$ is calculated based on the day of the month when the original energy demand during the on-peak layover period is maximum. Let $\mathrm{ED}_{org,on}(d) = \sum_{16\,\mathrm{h}}^{t_f^j}(L_{org}(d,t) \times \Delta t)$ be the original energy demand during the on-peak EV layover period on "d" day of the month and $\max \mathrm{ED}_{org,on}$ be the maximum $\mathrm{ED}_{org,on}(d)$ of all weekdays of the month, then the $\mathrm{OPDP_{V2B}}$ is formulated as

$$\mathrm{OPDP_{V2B}} = \frac{[\max \mathrm{ED}_{org,on} + \mathrm{ED}_{on}]}{(t_f^j - 16\,\mathrm{h})}. \tag{17b}$$

$\mathrm{NCDP_{V2B}}$ is calculated based on the day of the month when the original energy demand during the layover period is maximum, and is formulated as

$$\mathrm{NCDP_{V2B}} = \frac{\left[\max \mathrm{ED}_{org} + \mathrm{CD_{day}} - \mathrm{OPDP_{V2B}} \times \left(t_f^j - 16\mathrm{h}\right)\right]}{\left(16\,\mathrm{h} - t_i^j\right)}. \tag{17c}$$

The energy charges for V2B are formulated similarly to Eq. (16c), (16d) and (16e), with "V1G" subscripts being replaced by "V2B".

3.2.4.5 Implementation of the mathematical approximations for Jan 2019

Table 5. Comparison between optimization and analytical results for Jan 2019 for the 06:30-19:30 and 07:45-16:45 hours layover periods.

Metric	Symbol	Layover 06:30-19:30 hours		Layover 07:45-16:45 hours	
		Optimization	**Analytical**	**Optimization**	**Analytical**
Final V0G slope ($/kWh/day)	$\mathrm{Slope_{V0G}}$	9.6	9.6	9.6	9.6

Final V1G slope ($/kWh/day)	$\mathrm{Slope}_{\mathrm{V1G}}$	5.2	5.2	5.6	5.6
Final V2B slope ($/kWh/day)	$\mathrm{Slope}_{\mathrm{V2B}}$	5.2	5.2	5.6	5.6
V1G threshold daily charging demand (kWh)	$\mathrm{CD}_{\mathrm{day,thr,V1G}}$	216	211	144	114
V2B threshold daily charging demand (kWh)	$\mathrm{CD}_{\mathrm{day,thr,V2B}}$	168	46	144	33
Final monthly offset ($) between V1G and V2B		156.4	164.6	97.9	99.0

Table 5 shows a comparison between the optimization and analytically derived (Eqs. 12 through 17) V0G, V1G and V2B metrics for the 06:30-19:30 hours layover in Jan 2019. The final V0G, V1G and V2B slopes are predicted without error by the analytical method (Eq. (12)), because charging takes place exactly according to the strategy described in Section 3.2.4.1. The $\mathrm{CD}_{\mathrm{day,thr,V1G}}$ is predicted accurately analytically, and the difference between the optimization and analytical values occurs primarily because we increase the daily charging demand in multiples of 24 kWh for the optimization (see discussion of Fig. 3(c), where increasing the $\mathrm{CD}_{\mathrm{day}}$ from 192 to 216 kWh changes the off-peak layover period load from 109.0 to 109.5 kW and makes the on-peak period layover load constant at 96.5 kW. If the $\mathrm{CD}_{\mathrm{day}}$ were 211 kWh, both the off-peak and on-peak period layover loads would have been constant at 109.0 and 96.5 kW respectively, after which the excess charging demand is accommodated uniformly in the off-peak layover period). $\mathrm{CD}_{\mathrm{day,thr,V2B}}$ is underpredicted by the analytical method and gives only a lower bound of the actual daily threshold charging demand. $\mathrm{CD}_{\mathrm{day,thr,V2B}}$ is underpredicted because according to Eq. (14a) through (14c) the V2B EVs are assumed to discharge at their maximum capacity during the original NC and PP demand peaks, resulting in the off-peak and on-peak loads becoming constant at their reduced peaks, without regard for the EV final SOC constraints. The Offset is calculated analytically with high accuracy with the maximum error being less than 6% with respect to the optimization value. The error is caused due to the approximate energy (in Eq. (16d) and (16e) of main text) and other charges, as the NC and PP demand charges are calculated accurately (not shown in Table 5).

For the layover period of 07:45-16:45 hours, Table 5 shows that for Jan 2019, the final V0G, V1G and V2B slopes are predicted exactly by the analytical method. The $\mathrm{CD}_{\mathrm{day,thr,V1G}}$ is underpredicted analytically, and the difference between the optimization and analytical values occurs primarily because above 114 kWh of daily charging demand, additional charging takes place exclusively in the off-peak period, but the charging is non-uniform; only at approximately 144 kWh of daily charging demand, the additional charging demand is spread out uniformly over the off-peak period leading to a constant slope. Like the 06:30-19:30 hours layover, the Offset is calculated analytically with high accuracy with maximum error being about 1.2%.

3.2.4.6 Interpretation of the total electricity charges versus daily EV charging demand curve

Figure 5(a) shows that for Jan 2019 V0G charging for the 06:30-19:30 hours layover, the slope becomes constant at $9.6/kWh/day with increasing daily charging demand above 24 kWh. These costs should not be confused with electricity (energy) costs per kWh charged. Since there are 23 weekdays in the month when EV charging occurs, $9.6/kWh/day = $0.42/kWh/month; in other words, the average electricity cost per kWh charged is 42 cents. Since all graphs are presented in kWh of daily EV charging (energy) demand, we chose to continue to report results using the $/kWh/day metric.

For V1G charging, the slope is initially constant at $2.5/kWh/day until 144 kWh of daily charging demand, because charging takes place in the off-peak layover period only, without increasing the NC demand peak over the original. The slope until 144 kWh of daily charging demand can be found from Eq. (12), with $\Delta\mathrm{NCDC} = 0$. Finally, the V1G slope becomes constant at \$5.2/kWh/day with additional daily charging demand above 216 kWh. For V2B charging, the slope is negative initially, then becomes positive and increases to \$5.1/kWh/day with increasing daily charging demand up to 168 kWh. With additional charging daily demand above 168 kWh, the slope becomes constant at \$5.2/kWh/day, resulting in parallel V2B and V1G curves above 216 kWh of daily charging demand. The slope of the V2B electricity charges curve increases faster than V1G from 48 to 216 kWh of daily charging demand because the addition of daily charging demand (from 48 kWh to 216 kWh) results in a greater increase of the NC demand peak for V2B as compared to V1G (see Table 4 V1G and V2B NC and PP demand peaks for the 06:30-19:30 hours layover). For example, for 72 to 216 kWh of daily charging demand, the PP demand peak remains constant for V1G at 96.5 kW and at 82.4 kW for V2B and does not affect the slope of electricity costs versus daily energy demand curve. On the other hand, the NC demand peak costs increase faster for V2B resulting in a faster increasing slope of electricity costs versus daily energy demand for V2B compared to V1G.

Figure 5(b) shows that for the entire year 2019, the slope of V0G charging for the 06:30-19:30 hours layover, becomes constant at \$114.9/kWh/day above 48 kWh of daily charging demand. For V1G charging, the slope is \$29.4/kWh/day until 120 kWh of daily charging demand, then increases, and becomes constant at \$62.2/kWh/day with daily charging demands above 240 kWh. For V2B charging, the slope is negative up to a daily charging demand of 48 kWh, then becomes positive and increases, and finally becomes constant at \$62.2/kWh/day above 216 kWh of daily charging demand, resulting in parallel V2B and V1G curves above 240 kWh of daily charging demand.

3.3 Overall results for all buildings

To explain the building-to-building differences in the electricity charges associated with EV charging, in this Section we discuss the results for all buildings for one sample initial and final SOC combination (50 & 90% respectively) and one layover period (06:30-19:30 hours). The initial and final SOC combination is chosen as 50 & 90% respectively to be consistent with the rest of the paper.

Figure 6 shows that for all buildings, V0G incurs the highest EV charging costs (the difference between post and pre-EV charging building electricity costs), followed by V1G and V2B. For V0G charging, all charging takes place between 06:30-10:15 hours (see Section 3.2.1). The difference between the V0G EV charging costs from building-to-building is driven by differences in the NCDC. The monthly increase in the NCDC for a building depends on two factors: (a) The intersection of the original NC demand peak time with the time of V0G charging. If the original NC demand peak falls within the V0G charging time, the post-EV charging new NC demand peak increases at the charging power of the EV; (b) If there is no intersection in (a), the difference between the original NC demand peak and the maximum original load in the month during the V0G charging time. If the original NC demand peak time falls outside the V0G charging time, and the lower the difference between the original NCDP and the maximum original load in the month in the V0G charging time, the higher the chance that a particular number of EV will increase the NCDP. For V0G, most buildings show EV charging cost increases consistent with 6.6 kW per EV of increased NCDP for daily EV energy demand over 100 kWh, but building XIII shows smaller cost increases as the original NC demand peak is much larger than the maximum load during the EV charging time.

Building XIII is also the main outlier for V1G and V2B as the charging can be spread over the layover period such that the building load stays below the original peak demand even for 432 kWh of daily EV charging demand. Therefore, electricity cost increases for building XIII reflect only the additional energy charges and there is no demand charge contribution. For V1G and V2B charging at the other buildings, the variation between the EV charging costs from building-to-building is driven by NCDC, OPDC (only for V2B), and off and on-peak energy costs. For V1G, the electricity costs initially increase with a slope that is consistent with only energy charges from off-peak charging, but eventually transition to a slope consistent with energy and demand charges from constant charging during the off-peak period. The transition occurs mostly between 100 to 400 kWh of charging demand, depending on the building. The smaller the difference between the original demand peaks and the off and on-peak layover period mean loads, the higher the chance that a particular number of EVs will increase the peak demand charges.

For V2B, the final slopes are consistent with the V1G slopes and the ordering of the EV charging costs for high daily EV energy demand is also consistent with V1G. The lower envelope of the initial decrease in V2B electricity costs is consistent with a decrease of 6.6 kW in both NC and PP demand charges, i.e. EVs discharging at full power. Depending on the building, the slope is maintained for up to 3 EVs (72 kWh of charging demand), is followed by a slower decrease (less than 6.6 kW decreases in NC and PP demand charges), and eventually becomes positive as demand charge reductions become infeasible and the energy costs increase, and eventually the demand charge increases dominate. The intersection of the original demand peak times along with the layover period plays a large role for V2B. Specifically, if the original demand peak times do not fall within EV layover time, V2B charging cannot reduce costs.

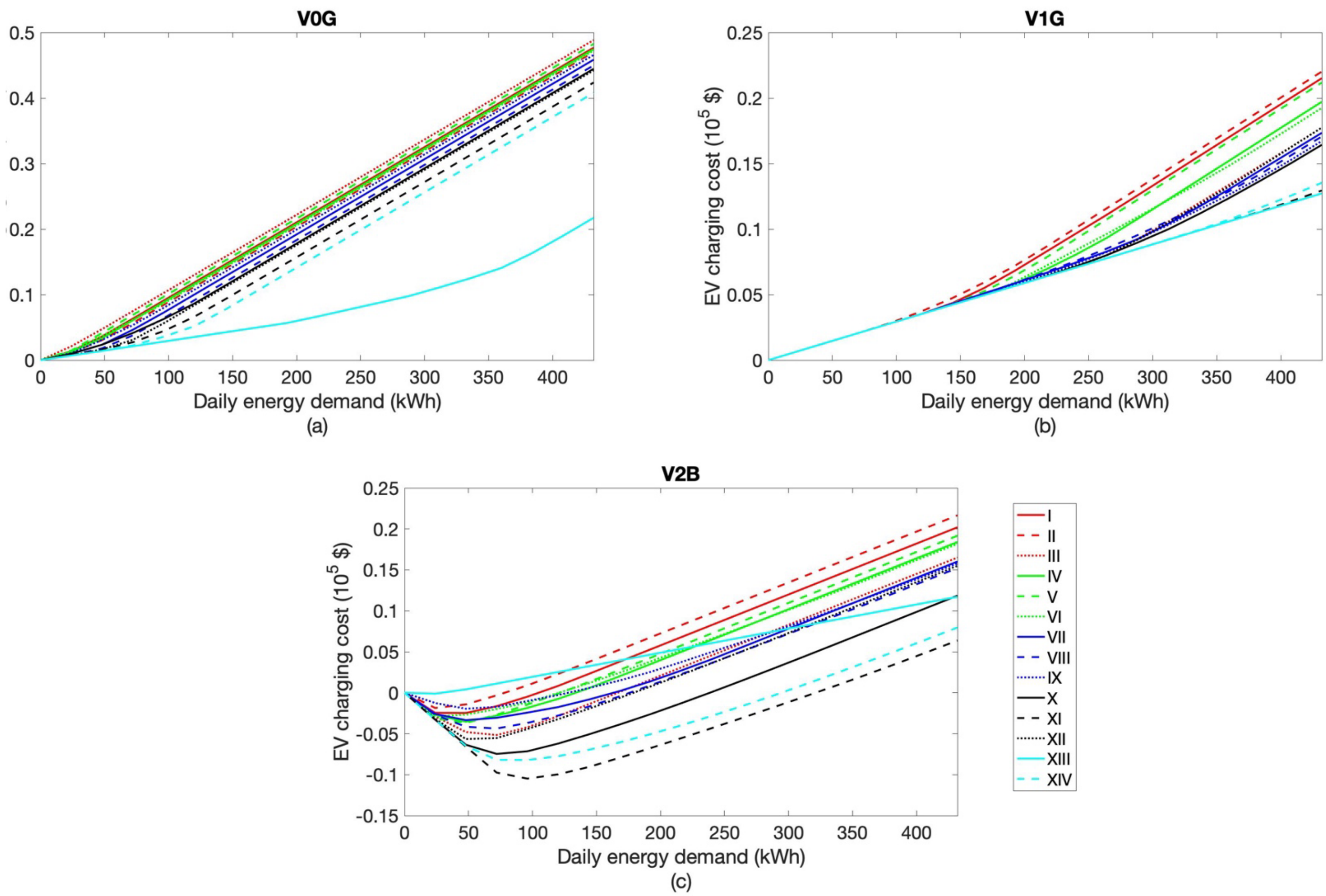

Figure 6. EV charging cost versus total daily EV energy demand for all buildings for the 06:30-19:30 hours layover for the entire year 2019 for initial and final SOC of 50 & 90% respectively for (a) V0G charging, (b) V1G charging, and (c) V2B charging. The legend represents the building number.

The results for the total electricity charges (not shown graphically) elucidate that for all three charging strategies, generally, as the mean original real load (proxy for the original load of the buildings) of the buildings increase (Table 2), the total electricity charges also increase, as the demand and energy charges are higher for a building with higher original load.

Table 6 shows the optimal number of V2B EV charging stations to be installed at a building such that the original (pre-EV) electricity costs are not exceeded. Generally, for a given month, the larger the difference between the original NCDP & the mean load in the off-peak period, and the original OPDP & the mean load in the on-peak period (as quantified in Eq. (18), the more V2B EV charging reduces the NCDC and PPDC. It then follows that the greater the NCDC and PPDC savings, the higher the number of optimal V2B charging stations for a building. Hence, in Table 6, we present the optimal number of V2B charging stations as a function of a metric w, which weights the difference in original peak and mean loads by the off and on-peak layover times averaged over the 12 months in 2019. w is formulated as

$$w = \text{mean}\left\{\sum_{\text{month}=1}^{\text{month}=12}\left[\left(\text{NCDP}_{org} - \text{mean}\left\{\left(\sum_{d=1}^{d=m}\sum_{t=0}^{t=16\text{ h}-\Delta t} L_{org}(d,t)\right) + \left(\sum_{d=1}^{d=m}\sum_{t=21\text{ h}}^{t=24\text{ h}-\Delta t} L_{org}(d,t)\right)\right\}\right) \times \frac{(16\text{ h}-t_i^j)}{(t_f^j-t_i^j)} + \left(\text{OPDP}_{org} - \text{mean}\left\{\sum_{d=1}^{d=m}\sum_{t=16\text{ h}}^{t=21\text{ h}} L_{org}(d,t)\right\}\right) \times \frac{(t_f^j-16\text{ h})}{(t_f^j-t_i^j)}\right]\right\}, \tag{18}$$

where d takes the value of the date index of the month for only weekdays (when EV charging occurs). The month argument is dropped from NCDP, OPDP and L_{org} for simplicity of presentation of Eq. (18).

Table 6. Optimal number of V2B EV charging stations by building

Buildings arranged in increasing order of w (Eq. 18)	w	Optimal # of V2B charging stations
II	20.8	3
I	29.2	4
III	38.2	6
VII	40.6	6
IX	42.4	5
V	44.0	5

IV	44.7	5
VII	44.9	6
VI	48.0	5
XII	53.6	7
X	81.6	9
XI	104.0	13
XIII	114.4	1
XIV	134.2	12

Table 6 shows that generally as w increases, the optimal number of V2B charging stations also increases. The optimal number of V2B charging stations for building XIII is an outlier because, for the EV layover period (06:30-19:30 hours) considered, for most of the months (9 out of 12) its NCDP_{org} occurred outside the layover period and for the remaining 3 months it occurred in the PP period, giving the V2B EVs little chance to reduce the NCDP. For some of the months, the OPDP_{org} of building XIII also occurred out of the layover period, further preventing load shifting and electricity cost reduction by V2B.

3.4 Sensitivity analyses

Section 3.2 presented a case study for the idealized uniform commuter EV fleet for initial and final SOC of 50 and 90% respectively for the 06:30-19:30 hours layover for building V for the year 2019. In this Section, we carry out sensitivity analyses based on the initial and final SOCs of 45 & 85%, 40 & 80%, 50 & 85%, and 50 & 80%, to present the effect of varying the initial and final SOCs on the NC and PP demand costs, energy costs, and total electricity costs for both layover periods for the year 2019. The effect of varying initial and final SOCs on total electricity costs is presented graphically for building V for 2019 in this Section (consistent with the rest of the paper), while the variation of all metrics (NC and PP demand costs, energy costs and total electricity costs) for the SOC combinations with the same daily charging energy demand, for all buildings for both the layover periods is presented in Tables S1, S2 and S3 of the Supplementary material.

If the final SOC is reduced below 90% (note that for our analyses the maximum and minimum SOC of the EV battery is 20 and 90% respectively), it is possible for the V2B EVs to discharge immediately before disconnecting and therefore further discharge during the on-peak period. In Section 3.2.3, typically the net V2B charging demand during the on-peak period was zero or positive (if charging up to 90% during the off-peak period was not optimal, resulting in net charging during the on-peak period), while in this Section (for final SOCs below 90%) the net V2B charging demand during the on-peak period is expected to be negative (net discharging).

Figures 7(a) and 7(c) show results for EVs having different initial and final SOCs but the same daily charging energy demand for the 06:30-19:30 hours and 07:45-16:45 hours layover, respectively. For a particular layover period, the V0G and V1G total electricity charges are the same if the daily charging energy demand of the EVs is the same, as the V0G and V1G EV charging costs do not depend on the final SOC because they do not have the ability to discharge. V2B EVs make use of the lower final SOC, to shift demand from the on-peak period to the off-peak period resulting in cost savings, as the on-peak period has higher energy charge rates and additional demand charges over the off-peak period. The V2B total electricity costs decrease for both layover periods as the final SOC decreases from 90 to 80% (with initial SOC decreasing from 50 to 40%) because the smaller the final SOC the more flexibility for discharging during the on-peak period. The strategy of V2B EVs to discharge more during the on-peak period as final SOC decreases from 90 to 80% is accompanied by more charging during the off-peak period, which ultimately leads to net total electricity cost savings, i.e., the decrease in the on-peak periods costs is greater than the increase in the off-peak period costs.

Figures 7(b) and 7(d) correspond to EVs having different final SOCs (with initial SOC fixed at 50%) and thus different daily charging energy demand for the 06:30-19:30 hours and 07:45-16:45 hours layovers, respectively. The total electricity charges for both layover periods for all charging strategies are smallest for a final SOC of 80% and increase as the final SOC increases to 85 to 90%. The smaller cost for V0G and V1G, for lower final SOCs is due to the smaller total charging energy demand (as initial SOC is fixed at 50%). The V1G costs decrease more than V0G because, as the final SOC (and thus charging demand) decreases, the V1G average load (and therefore incremental NCDC) is proportional to the charging demand per Eq. (16b), as opposed to V0G which charges without regard for the original load curve and costs. For V2B, in addition to the former point, there is an added benefit of more discharging potential during the on-peak period when the final SOC is lower than 90%. The sensitivity analyses (comparison between Figs. 7(a) & 7(c), and 7(b) & 7(d)) also show that the shorter layover period of 07:45-16:45 hours leads to higher total electricity charges compared to the longer layover period of 06:30-19:30 for all charging strategies for any particular initial and final SOC combination.

Tables S1, S2 and S3 of the Supplementary material present the results with initial and final SOC of 50 & 90%, 45 & 85%, and 40 & 80%, respectively.

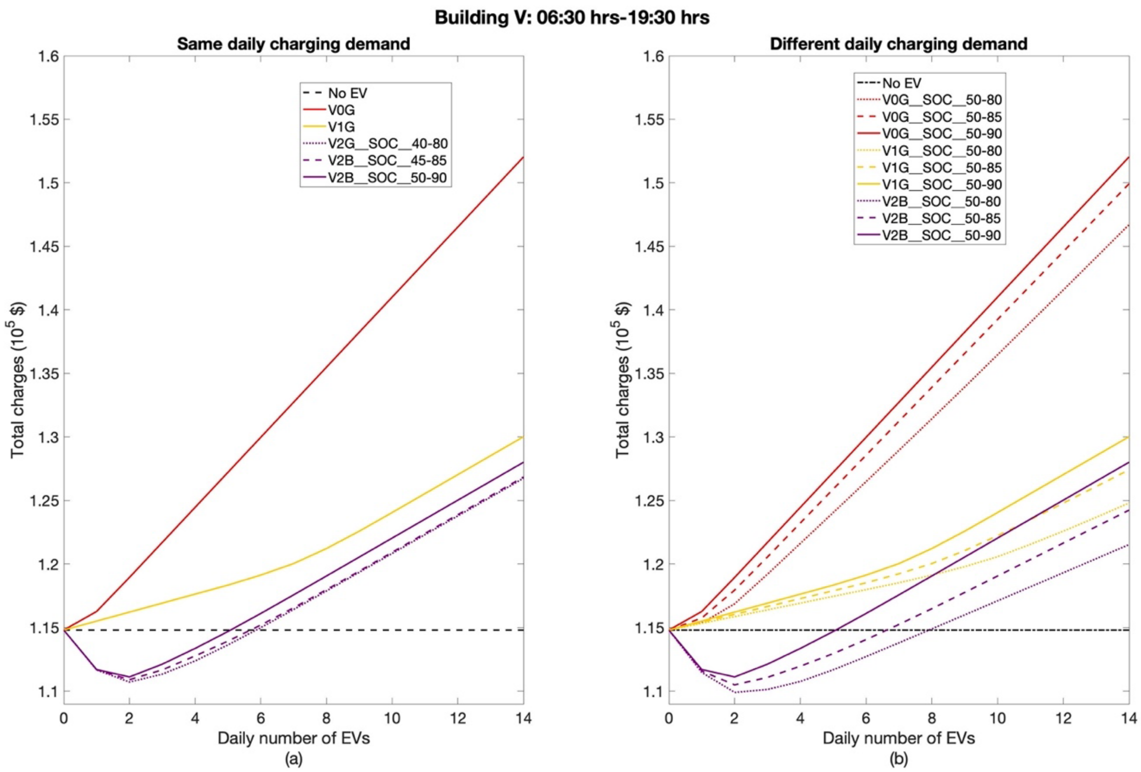
Building V: 06:30 hrs-19:30 hrs
Same daily charging demand
No EV
V0G
V1G
V2G__SOC__40-80
V2B__SOC__45-85
V2B__SOC__50-90
Total charges (10^5 $)
Daily number of EVs
(a)
Different daily charging demand
No EV
V0G__SOC__50-80
V0G__SOC__50-85
V0G__SOC__50-90
V1G__SOC__50-80
V1G__SOC__50-85
V1G__SOC__50-90
V2B__SOC__50-80
V2B__SOC__50-85
V2B__SOC__50-90
Total charges (10^5 $)
Daily number of EVs
(b)

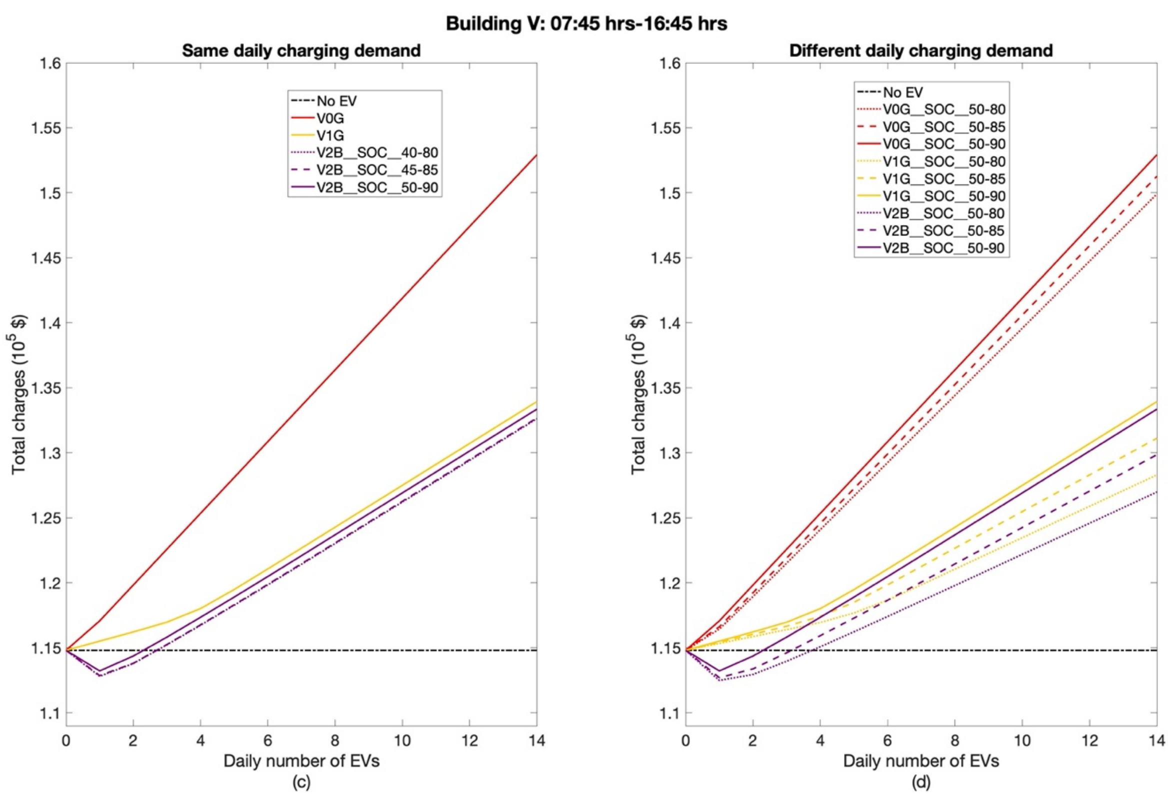
Building V: 07:45 hrs-16:45 hrs
Same daily charging demand
No EV
V0G
V1G
V2B__SOC__40-80
V2B__SOC__45-85
V2B__SOC__50-90
Total charges (10^5 $)
Daily number of EVs
(c)
Different daily charging demand
No EV
V0G__SOC__50-80
V0G__SOC__50-85
V0G__SOC__50-90
V1G__SOC__50-80
V1G__SOC__50-85
V1G__SOC__50-90
V2B__SOC__50-80
V2B__SOC__50-85
V2B__SOC__50-90
Total charges (10^5 $)
Daily number of EVs
(d)

Figure 7. Total electricity charges versus daily number of EVs for the for the entire year 2019 for the layover period (a, b) 06:30-19:30 hours, and (c, d) 07:45-16:45 hours, at building V for (a, c) same daily charging demand with initial and final SOCs being 40 & 80%, 45 & 85%, and 50 & 90%, respectively, and (b, d) different daily charging demand with initial and final SOCs being 50 & 80%, 50 & 85%, and 50 & 90%, respectively. The legends in the figure correspond to the charging strategies along with their initial and final SOCs. For example, V0G__SOC__50-80 indicates V0G charging with initial and final SOC of 50 and 80% respectively.

3.5 A realistic case using historical data

A realistic case study is carried out using historical EV data of charging records available from ChargePoint at UC San Diego. The relevant historical data used in this analysis are the time of EV connection and disconnection, end of charging, charging demand, initial and final SOC (for a subset of events only), EVSE IDs, and port type (Level 2 (L2) and Direct Current Fast Chargers (DCFC)). For a data sample, see Ref. 17. Originally the EVs were charged with the V0G charging strategy, which did not make use of the flexibility afforded by the complete layover time, i.e., originally the EVs charged too quickly when more suitable later times were available for charging.

The EV battery capacity is required to understand the EV discharging or delayed charging opportunities. The ChargePoint data does not (directly) contain the EV (rated) battery capacity data, but the initial and final SOCs are given for 5,754 out of the total of 168,122 charging events that occurred between March 15, 2016 and August 4, 2020. For the 5,754 events, EV battery capacity is calculated as $\mathrm{BC}^j = \frac{\mathrm{ED}^j}{\left(\mathrm{soc}_f^j - \mathrm{soc}_i^j\right)}$. We observe an anomaly for five charging events, for which the calculated battery capacity is above 200 kWh. We remove these five datapoints from our analysis as most EVs have a battery capacity below 200 kWh [22]. To impute the missing EV battery capacity for the remaining 162,368 charging events, we randomly draw data from the calculated battery capacity (5,749 events).

Following these calculations, we set the following charging constraints: (i) The missing final SOC is initially imputed by randomly drawing from the given "valid" final SOCs. (ii) The missing initial SOC is calculated from the final SOC, energy demand, and the EV battery capacity data as $\mathrm{SOC}_i^j = \mathrm{SOC}_f^j - \frac{\mathrm{ED}^j}{\mathrm{BC}^j}$. (iii) If the SOC_i^j is calculated as less than 0% by (ii), it is corrected and fixed at 0% as the SOC range for the analyses is 0-100%. Correspondingly the battery capacity is again updated for that EV as $\mathrm{BC}^j = \frac{\mathrm{ED}^j}{\left(\mathrm{SOC}_f^j - \mathrm{SOC}_i^j\right)}$, for which $\mathrm{SOC}_i^j = 0$. (iv) The maximum charging and discharging rate of EVs is 7.2 kW for L2 and 50 kW for DCFC. The input variables for the realistic analysis are shown in Table 7.

Table 7. Inputs for the realistic case study

Metric	Symbol	Value
Maximum charging rate of L2 chargers	$\max \mathrm{EV}_{\mathrm{L2}}^j$	7.2 kW
Maximum charging rate of DCFC chargers	$\max \mathrm{EV}_{\mathrm{DCFC}}^j$	50 kW
Data sampling interval	Δt	1 hour

Table 7 shows that the data sampling interval is chosen as 1 hour instead of 15 minutes as for the uniform fleet Case study (A), because of unreasonably long run-times for 15-minute timesteps in the realistic case study. The actual time of EV connection and disconnection is mapped onto the hourly scale, depending on the minute of the hour of the connection or disconnection from the charging station. Initially the EV connection and disconnection time is rounded up to the nearest hour. For example, if an EV originally connects at 00:29 hours and disconnects at 1:35 hours on the same day, it is assumed in our algorithm that the EV connects at 00:00 hours and disconnects at 02:00 hours on that day. After the initial rounding to the nearest hour, a correction is implemented for the EVs that have the same connection and disconnection time. In these cases, the connection time is assumed to be the beginning of the hour and the disconnection time is assumed to be the end of the hour. For example, if an EV originally connects at 16:45 hours and disconnects at 16:59 on the same day, rounding to the nearest hours would cause both the connection and disconnection time to be 17:00 hours on that day. The correction assumes that the EV connects at 16:00 hours and disconnects at 17:00 hours.

Our analysis is carried out for 5 weekdays of February 2020. The EV charging stations are located in the Osler Parking Structure. The Osler Parking Structure is chosen for the analysis as it consists of 16 L2 (with 14 being in use for this analysis) and 2 DCFC fast chargers which is representative of an EV charging station installation infrastructure at a single location [23]. The total load of the Osler Parking Structure EV charging stations is mapped to a single building having 0 original load, i.e. the optimized EV load is assumed to equal the final building net load. As per the original V0G charging schedule the NC demand peak occurs on Feb 14, 2020, we choose the weekdays Feb 10 to Feb 14, 2020 for the analyses, so that the NC demand peak is representative for the entire month of February 2020. 338 charging events occur from Feb 10 through 14, 2020, with average layover, charging time, and energy demand of 3 hour 29 minutes, 1 hour 38 minutes, and 9.8 kWh respectively, with 256 events occurring at L2 chargers and 82 events occurring at DCFC chargers. 251 charging events at L2 chargers have charging flexibility, whereas all the events at DCFC chargers have charging flexibility (i.e. $(t_f^j - t_i^j) \times \max \mathrm{EV}^j > \mathrm{ED}^j$). Since there are some inconsistencies in the dataset, the final EV energy demand is corrected for 5 L2 charging events by charging at maximum power during the entire layover period (refer to Eq. (9)). The objective function minimized is Eq. (1), with the cost components (NC and PP demand charges, energy charges, and other charges) being adjusted for 5 days instead of the entire month.

Figure 8(a) shows the timeseries for February 10 through February 14, 2020 for all 3 charging strategies. Figure 8(b) shows the NC and PP demand charges along with the total electricity costs for our analysis. The total electricity costs incurred by the EVs based on the original V0G charging, and the optimized V1G and V2G charging are \$5,694, \$3,402, and \$2,598 respectively. The results show that the V2G and V1G charging strategies results in 54.4 and 40.3% total electricity cost savings, respectively over the original V0G charging schedule.

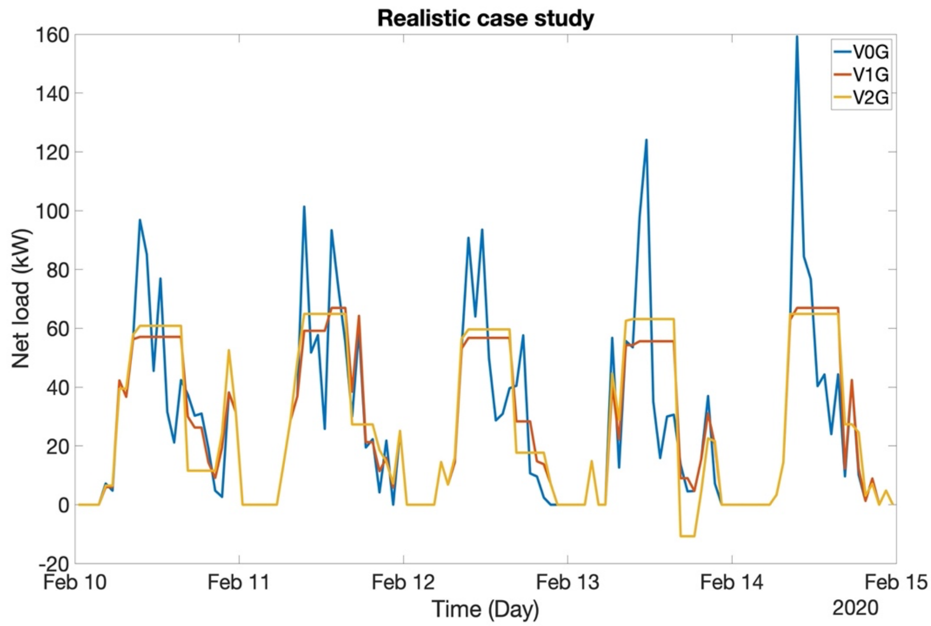

(a)

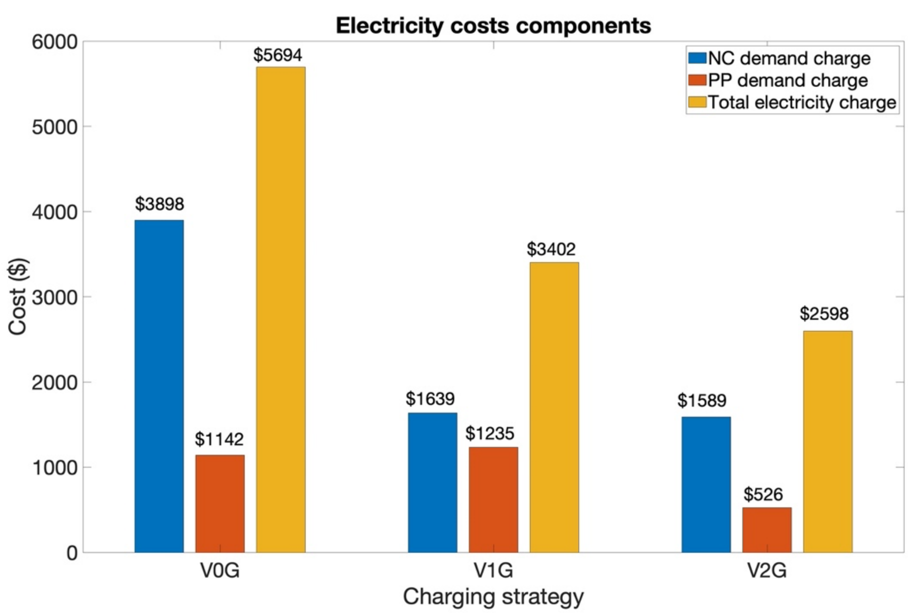

(b)

Figure 8. (a) Original (V0G) and optimized net load (= EV charging) timeseries analysis, and (b) Electricity cost components for the 3 charging strategies, for the realistic case study

from February 10 through 14, 2020. The total electricity charges in (b) differ from the sum of the NC and PP demand charges because they also include energy charges.

4. Conclusions

We carry out a techno-economic analysis of three different types of workplace EV charging strategies (V0G, V1G and V2B) in 14 commercial buildings with real load profiles. We primarily base our analysis on an idealized uniform EV commuter fleet case study with a layover period of 06:30-19:30 hours for the year 2019.

V0G incurs the highest year-around electricity costs followed by V1G and V2B. For V0G, the building-to-building difference in EV charging costs depends on the intersection of the original NC demand peak time with the EV charging time, and the difference between the original NC demand peak and the maximum original load during the EV charging time. For V2B, the building-to-building difference in EV charging costs depends on the intersection of the original NC and PP demand peak times with the EV layover time. For V1G and V2B the building-to-building difference depends on the difference between the original demand peaks and the mean original load during the on and off-peak layover periods.

The V1G and V2B total electricity costs initially diverge with increasing daily charging demand (or number of EV charging stations) and then become parallel to each other. As the daily charging demand increases, the cost savings of V2B charging over V1G reduce and the V2B charging costs exceed the original (pre-EV) costs. A longer layover period generally leads to more cost savings over a shorter layover period for V1G and V2B, as the charging is spread out over a longer duration for V1G, while for V2G there is an additional flexibility of shifting on-peak loads to off-peak periods. Correspondingly, a longer layover period also leads to a higher number of optimal V2B charging stations (the number of V2B charging stations to be installed at a building such that its operating electricity costs do not exceed the pre-EV original electricity costs), as compared to a shorter layover period. Generally, with increasing difference between the original NCDP & mean off-peak period load and the original OPDP & mean on-peak period load, weighed over the off-peak and on-peak layover times respectively, the optimal number of V2B charging stations increases.

Sensitivity analyses based on changing both initial and final SOC of EVs while keeping the energy demand constant for all the buildings for both layover periods show that, as the final SOC decreases from 90 to 80% (with the initial SOC decreasing from 50 to 40%), the total electricity costs remain the same for V0G and V1G, while for V2B the total electricity costs decrease because of the additional flexibility of discharging during the on-peak period.

A realistic case study based on historical data for 5 high charging demand weekdays in February 2020 for 14 EV charging stations shows that the V2G and V1G charging strategy results in 54.4% and 40.3% total electricity cost savings respectively over the original V0G charging schedule.

While the results discussed so far were all based on convex optimization, we also provided general equations that allow estimating V1G and V2B benefits based on a pre-EV building load profile and EV and tariff data. Although the number of V2B charging stations such that the original (pre-EV) operating electricity bill is not exceeded cannot be predicted exactly without carrying out the convex optimization, we provided a framework (using Eq. (18), in conjunction with Table 2 and Table 6) to approximate the optimal number of V2B charging stations without carrying out the convex optimization, which may be of interest to building owners.

One of the limitations of this study is the assumption of 100% charging/discharging efficiency for the EVs. In reality, each time an EV charges/discharges there are costs due to energy losses and battery degradation. Therefore, if the losses were considered, the V2G/V2B charging economic benefits, which depend on more charging/discharging cycles, would reduce. Another limitation of the study is that uncertainties in layover periods and battery capacity (which may occur due to ageing) are not considered. Future work will focus on tackling these limitations to make the study more robust and accurate and increase its applicability to more realistic scenarios.

Supplementary material

See the Supplementary material attached alongside the manuscript, for some Results and discussions which could not be discussed in the main text due to space limitations. Section 1.1 of the Supplementary material expands upon the uniform fleet V0G and V2B analysis already presented in Section 3.2.1 and 3.2.3 of the main text respectively for building V for the 06:30-19:30 hours layover. Section 1.2 of the Supplementary material presents the V0G, V1G, and V2B analyses for building V for the 07:45-16:45 hours layover. Section 1.3 of the Supplementary material presents a hypothetical case study demonstrating the ability of V2G/V2B EVs to save electricity costs by shifting load from the on to the off-peak layover period. Section 1.4 of the Supplementary material elucidates on the general applicability of the optimization model and the trend of total electricity charges versus total daily EV energy demand curve for electricity tariff structures other than those used in our paper. Tables S1, S2 and S3 of the Supplementary material present the effect of varying both the initial and final SOCs of the EVs on the NC and PP demand costs, energy costs and total electricity costs, while keeping the charging energy demand constant for the year 2019 for all buildings for both layover periods.

Data availability statement

The data that supports the findings of this study are available within the article and its supplementary material.

References

[1] EV Charging Stations Continued Strong Growth in Early 2020, NREL Report Shows | News | NREL n.d. https://www.nrel.gov/news/program/2020/ev-charging-stations-continued-strong-growth-in-early-2020-nrel-report-shows.html (accessed February 3, 2021).

[2] B. Aluisio, A. Conserva, M. Dicorato, G. Forte, and M. Trovato, Electr. Power Syst. Res. **152**, 295 (2017).

[3] Slide 1 | Enhanced Reader n.d. moz-extension://5a53ee4f-b368-6a4c-86ab-0e14814c9436/enhanced-reader.html?openApp&pdf=http%3A%2F%2Fwww.regen.co.uk%2Fwp-content%2Fuploads%2FRegen-V2G-Learnings-Sept-2019-v2.pdf (accessed February 4, 2021).

[4] M. Huda, K. Tokimatsu, and M. Aziz, Energies **13**, 1162 (2020).

[5] R. Shi, S. Li, P. Zhang, and K.Y. Lee, Renew. Energy **153**, 1067 (2020).

[6] M. Kiaee, A. Cruden, and S. Sharkh, J. Mod. Power Syst. Clean Energy **3**, 249 (2015).

[7] Z. Yang, K. Li, and A. Foley, Renew. Sustain. Energy Rev. **51**, 396 (2015).

[8] A. Schuller, B. Dietz, C.M. Flath, and C. Weinhardt, IEEE Trans. Power Syst. **29**, 2014 (2014).

[9] U. Datta, N. Saiprasad, A. Kalam, J. Shi, and A. Zayegh, Int. J. Energy Res. **43**, 1032 (2019).

[10] C. Zhou, Y. Xiang, Y. Huang, X. Wei, Y. Liu, and J. Liu, Energy Reports **6**, 509 (2020).

[11] V.C. Onishi, C.H. Antunes, and J.P. Fernandes Trovão, Energies **13**, 1884 (2020).

[12] X. Li, Y. Tan, X. Liu, Q. Liao, B. Sun, G. Cao, C. Li, X. Yang, and Z. Wang, Electr. Power Syst. Res. **179**, 106058 (2020).

[13] Saving Money by Understanding Demand Charges on Your Electric Bill, Cover Page n.d. https://www.fs.fed.us/t-d/pubs/htmlpubs/htm00712373/ (accessed April 2, 2022).

[14] G. Zhang, S.T. Tan, and G. Gary Wang, IEEE Trans. Smart Grid **9**, 4027 (2018).

[15] Y. He, Z. Song, and Z. Liu, Sustain. Cities Soc. **48**, 101530 (2019).

[16] N. Qin, A. Gusrialdi, R. Paul Brooker, and A. T-Raissi, Transp. Res. Part A Policy Pract. **94**, 386 (2016).

[17] S. Silwal, C. Mullican, Y.-A. Chen, A. Ghosh, J. Dilliott, and J. Kleissl, J. Renew. Sustain. Energy **13**, 025301 (2021).

[18] M. Grant and S. Boyd, CVX: Matlab Software for Disciplined Convex Programming | CVX Research, Inc. n.d. http://cvxr.com/cvx/ (accessed October 6, 2021).

[19] M.C. Grant and S.P. Boyd, Lect. Notes Control Inf. Sci. **371**, 95 (2008).

[20] How Long Does It Take to Charge an Electric Car? | Pod Point n.d. https://pod point.com/guides/driver/how-long-to-charge-an-electric-car (accessed June 30, 2021).

[21] What's the Difference Between EV Charging Levels? - FreeWire Technologies n.d. https://freewiretech.com/difference-between-ev-charging-levels/ (accessed September 16, 2021).

[22] EVs Explained: Battery Capacity, Gross Versus Net n.d. https://www.caranddriver.com/features/a36051980/evs-explained-battery-capacity-gross-versus-net/ (accessed September 5, 2021).

[23] Alternative Fuels Data Center: Electric Vehicle Charging Station Locations n.d. https://afdc.energy.gov/fuels/electricity_locations.html#/find/nearest?fuel=ELEC&location=La Jolla&page=2 (accessed September 5, 2021).